University of Szeged
Albert Szent-Györgyi Medical School
Doctoral School of Theoretical Medicine

HUN-REN Biological Research Centre
Institute of Biophysics
Neurovascular Unit Research Group

Ageing-related microinfarct-induced alterations in contractile protein expression in brain pericytes

Ph.D. thesis

Fanni Győri

Supervisor:
Imola Wilhelm M.D., Ph.D.

Szeged
2025

Table of contents

I. List of publications related to the dissertation

Győri, F., Mészáros, Á., Krecsmarik, M., Molnár, K., Balta, C., Hermenean, A., Farkas, A. E., Krizbai, I. A., & Wilhelm, I. (2025). Expression of alpha smooth muscle actin decreases with ageing and increases upon lumen obstruction in mouse brain pericytes. *GeroScience*, 47(2), 2525–2540. https://doi.org/10.1007/s11357-024-01429-0
D1, IF: 5.4 (2024)

Wilhelm, I., **Győri, F.**, Dudás, T., Nagy, V., Shreeya, T., Krecsmarik, M., Farkas, A. E., Fazakas, C., Krizbai, I. A. (2025). Eppur si muove: The dynamic brain pericyte (manuscript has been accepted for publication in *Fluids and Barriers of the CNS*)

II. Other publications

Sere, P., Zsigri, N., Raffai, T., Furdan, S., **Győri, F.**, Crunelli, V., & Lőrincz, M. L. (2021). Activity of the lateral hypothalamus during genetically determined absence seizures. *International journal of molecular sciences*, *22*(17), 9466. https://doi.org/10.3390/ijms22179466
D1, IF: 6.208

Molnár, K., Mészáros, Á., Fazakas, C., Kozma, M., **Győri, F.**, Reisz, Z., Tiszlavicz, L., Farkas, A. E., Nyúl-Tóth, Á., Haskó, J., Krizbai, I. A., & Wilhelm, I. (2020). Pericyte-secreted IGF2 promotes breast cancer brain metastasis formation. *Molecular oncology*, *14*(9), 2040–2057. https://doi.org/10.1002/1878-0261.12752
D1, IF: 6.603

Haskó, J., Fazakas, C., Molnár, K., Mészáros, Á., Patai, R., Szabó, G., Erdélyi, F., Nyúl-Tóth, Á., **Győri, F.**, Kozma, M., Farkas, A. E., Krizbai, I. A., & Wilhelm, I. (2019). Response of the neurovascular unit to brain metastatic breast cancer cells. *Acta neuropathologica communications*, *7*(1), 133. https://doi.org/10.1186/s40478-019-0788-1
D1, IF: 6.270

Nyúl-Tóth, Á., Mészáros, Á., **Győri, F.**, Wilhelm, I., & Krizbai, I. A. (2018). A vér-agy gát területi heterogenitásainak vizsgálata emberben és egérben [Analysis of regional heterogeneities of the blood-brain barrier in humans and mice]. *Bulletin of medical sciences / Orvostudományi értesítő*, *91*(1), 26–36. http://doi.org/10.2478/orvtudert-2018-0005

III. List of abbreviations

AD = Alzheimer's disease

BBB = blood–brain barrier

BSA = bovine serum albumin

CBF = cerebral blood flow

CCA = common carotid artery

CNS = central nervous system

DMEM/F-12 = Dulbecco's modified Eagle's medium/Nutrient Mixture F-12

ECA = external carotid artery

F-actin = filamentous actin

ICA = internal carotid artery

MeOH = methanol

MHC = myosin heavy chain

MLC = myosin light chain

mTORC1 = mammalian target of rapamycin complex 1 / mechanistic target of rapamycin complex 1

NVU = neurovascular unit

PBS = phosphate buffered saline

PDGF-B = platelet-derived growth factor B

PDGFR-β = platelet-derived growth factor receptor beta

PFA = paraformaldehyde

RIPA = radioimmunoprecipitation assay

ROCK = Rho-associated protein kinase

TBS-T = Tris-buffered saline containing 0.1% Tween-20

TGF-β = transforming growth factor-beta

VSMC = vascular smooth muscle cell

vWF = von Willebrand factor

α-SMA = alpha smooth muscle actin

IV. Introduction

1. The neurovascular unit

The brain has a well-organized vascular system maintaining homeostasis and energy supply through precise regulation of cerebral blood flow (CBF), which is required for proper functioning of neurons (1). This is coordinated by the neurovascular unit (NVU) composed of vascular cells (endothelial cells and mural cells, including smooth muscle cells and pericytes), as well as glial cells and neurons (2) (Figure 1a). Interactions between cells of the NVU modulate neurovascular coupling and maintain blood–brain barrier (BBB) functions, which are the most important roles of the NVU (3).

Neurovascular coupling, often called functional hyperaemia is a mechanism that matches regional blood flow to neuronal energy demand via regulating the intraluminal diameter of blood vessels (4). The process is initiated by the signals of activated neurons, mediated directly to vascular cells or indirectly by astrocytes, which increase the diameter of vessels, providing sufficient oxygen and nutrients to neurons (5,6).

Regulation of BBB is the other major function of the NVU. To maintain brain homeostasis, the BBB provides barrier and carrier functions at the level of the brain microvasculature. Cerebral endothelial cells connected by tight junctions form physical, transcellular, and enzymatic barriers, as well as express efflux pumps to prevent the entry of potentially toxic molecules into the brain. On the other hand, they have multiple substrate-specific transport systems to control the delivery of nutrients and essential molecules from the blood into the brain, and to remove metabolic waste from the brain into the blood (7). Besides endothelial cells, pericytes and astrocytes also have important roles in the formation of the BBB (2,7) (Figure 1b). Perivascular endfeet of astrocytes localize closely to the capillary wall, and contribute to barrier properties of cerebral endothelial cells by tightening the tight junctions and induction of polarized localization of transporters (7).

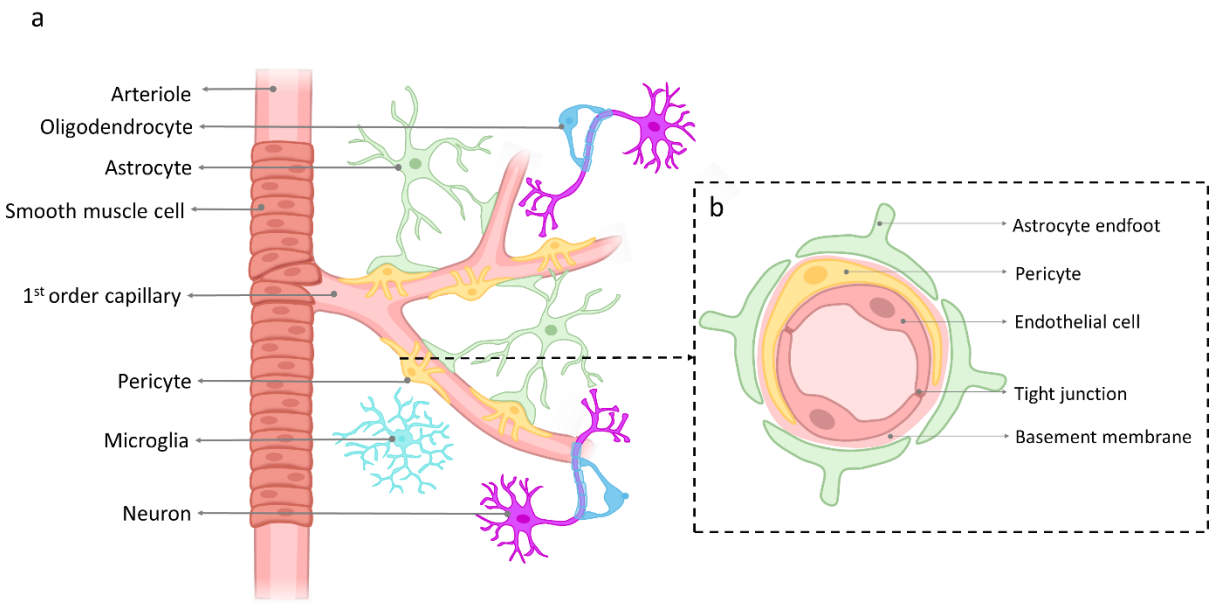

Figure 1. The neurovascular unit (NVU) and the blood–brain barrier (BBB).
a: Schematic representation of the NVU. Interactions between cerebral microvascular cells (endothelial cells and pericytes) and neural cells (neurons and glia) at the capillary level create the NVU, which regulates neurovascular coupling and maintains the integrity of the BBB. **b**: Cross section of a brain capillary showing the cellular components of the NVU.

2. Brain pericytes in physiological conditions

a. Definition and heterogeneity of brain pericytes

As part of the NVU, brain pericytes are located in the duplication of the basement membrane of microvessels, coming in close contact with cerebral endothelial and glial cells (Figure 1b). They were first characterized by Eberth and Rouget in the 1870s and named by Zimmerman in 1923 (8). They can be identified by their perivascular localization and expression of platelet-derived growth factor receptor beta (PDGFR-β), neural/glial antigen 2, and aminopeptidase N also known as CD13, which are the mostly used pericyte markers (9–11).

Pericytes have a bump-on-a-log morphology, so their stereotyped fusiform or ovoid body protrudes from the capillary wall (8). Furthermore, they extend processes along and around the capillaries with morphology that varies depending on their location within the microvasculature. At the arteriole end of the vasculature, their processes are more circumferential, at the mid-capillary level, they are more longitudinal; and at the venule end of capillary bed, they show stellate-like morphology (10,12).

However, pericytes differ not only in their morphology but in their protein expression as well. It has been recognized that pericytes with circumferential processes express more alpha

smooth muscle actin (α-SMA), a component of the actomyosin contractile machinery, while the ones with longitudinal processes contain less or no α-SMA (13).

Based on their morphology and protein expression, Grant *et al.* differentiated and named three types of pericytes (Figure 2). Ensheathing pericytes show higher coverage of the vessel and reside at the arteriole-capillary transition, *i.e.* between the 1st and 4th branch orders. They express high levels of α-SMA. Mesh pericytes cover the capillaries moderately, and they were identified mostly as α-SMA-negative. Thin-strand pericytes extend long, thin processes and lack α-SMA as well (12). Ensheathing and capillary pericytes (mesh and thin-strand) somata can be located at capillary junctions (junctional) or on intervening portions of the capillary (*en passant*) (10). Precise regulation of α-SMA expression in different pericyte subtypes has been later resolved (see: chapter IV.2.c).

b. Functions of brain pericytes

Brain pericytes play essential roles in numerous vascular functions. They regulate vessel formation and stabilization, the development and maintenance of the BBB, immune responses, and CBF.

In the regulation of angiogenesis (which means formation of new vessels from existing vessels) and vascular stability endothelial–pericyte contacts are necessary. Several ligand-receptor systems have been identified as important regulators in these processes. Among the key pathways are transforming growth factor-beta (TGF-β) and TGF receptors, angiopoietins 1 and 2 with their receptor Tie2, platelet-derived growth factor B signalling through PDGFR-β, and sphingosine-1-phosphate acting via its receptor, sphingosine-1-phosphate receptor 1 (14).

Pericytes have a crucial role in the formation and maintenance of the BBB as well. Daneman *et al.* showed that pericytes are required for the formation of tight junctions and for the reduction of vesicular transport in endothelial cells (15). It has also been documented that pericyte deficiency increases the permeability of the BBB (11).

Pericytes own several immune properties as well. During inflammation, they contribute to the recruitment of monocytes and lymphocytes by upregulating adhesion molecules, and to T-lymphocyte activation through their antigen-presenting activity (16,17). In addition, they release inflammatory mediators in response to lipopolysaccharide, suggesting that they have an important role in neuroinflammatory processes (18).

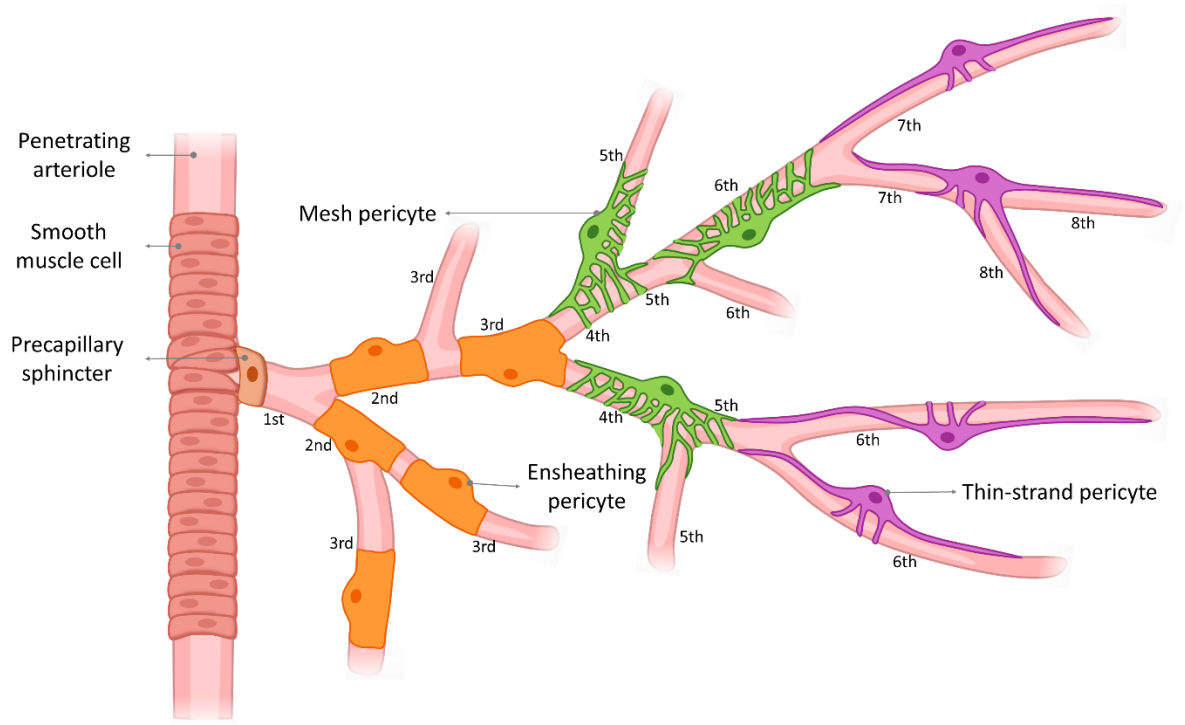

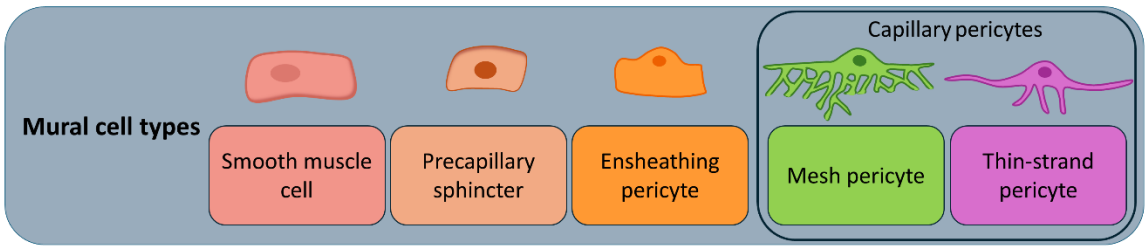

Pericyte types	Ensheathing	Mesh	Thin-strand
Location	1st-4th order capillary	>4th order capillary	
Morphology	relatively high vessel coverage	moderate coverage of the vessel	long, thin processes along the vessel
Fluoro-Nissl dye uptake	+/-	++++	
α-SMA expression	++++	+	
Calcium signalling	synchronized	unsynchronized	
Vasoconstriction	moderate contraction	slow contraction	
Vasodilation	rapid dilation during neuronal activity	small and delayed dilation during neuronal activity	

Figure 2. Mural cells of the brain vasculature.
Penetrating arterioles are surrounded by vascular smooth muscle cells (VSMCs). The transition zone between a penetrating arteriole and a first-order capillary may be marked by the presence of precapillary sphincter cells, typically found at the level of larger, proximal vessels. Low-order capillaries (first- to fourth-order), also referred to as pre-capillary arterioles or the arteriole-capillary transition zone, are encircled by ensheathing pericytes—previously termed transitional pericytes, arteriole-associated smooth muscle cells, or precapillary SMCs. Capillary pericytes, which express low levels of α-SMA, include mesh and thin-strand pericytes—terms that describe their distinct process morphology. These cells only partially cover the endothelial surface. Notably, ensheathing pericytes and capillary pericytes differ in their capacity to constrict and dilate blood vessels.

However, the most controversial role of brain pericytes is their involvement in regulation of CBF. Based on their perivascular location and morphology, it has been suggested that these cells might have contractile properties and regulate capillary blood flow (19). This idea is supported by anatomical aspects, such as the closeness of neuronal terminals and a high density of astrocytic endfeet, which transmit vasoactive signals from neurons to the vessels. Despite these suggestions, some studies failed to show the importance of pericytes in the coordination of blood flow. In these studies, arteriole smooth muscle cells were found to mediate functional hyperaemia (13). However, increasing number of researchers have demonstrated the significance of pericytes in neurovascular regulation. *In vivo* experiments revealed that pericytes actively relax to neuronal activation resulting earlier dilation of capillaries than arterioles (20). Additionally, optogenetic stimulation of brain capillary pericytes decreased lumen diameter and blood flow, suggesting pericytes' active role in vasoconstriction; however, with a slower kinetics than smooth muscle cells (21). Therefore, not surprisingly, degeneration of pericytes causes neurovascular uncoupling and reduce oxygen supply to the brain (22).

The controversy which surrounded the role of pericytes in CBF regulation arose from several issues. On the one hand, mural cells of the arteriole-capillary transition zone were defined inconsistently by different researchers (*e.g.* ensheathing pericytes were also called pre-capillary smooth muscle cells). Moreover, advanced optics and other tools to detect small changes of capillaries were lacking (23). On the other hand, the main issue was that contractile elements were undetectable in capillary pericytes.

c. Contractile properties of brain pericytes

Functional studies indicated that brain pericytes can promote dilation and vasoconstriction on the capillary level (20,21,24), but the contractile elements behind these processes remained unknown for a long time.

Motor proteins (myosin, kinesin, and dynein), which move along cytoskeletal filaments such as actin microfilaments and tubulin-formed microtubules, are responsible for generating the mechanical forces required for all types of cellular and intracellular movement. In smooth muscle and non-muscle cells, including pericytes from various organs, the actomyosin system—the main generator of mechanical forces in the cells—lacks sarcomeric organization and demonstrates high dynamism (25).

Globular actin, which polymerizes to form filamentous actin (F-actin), has six isoforms in mammals. These include the ubiquitously expressed cytoplasmic β-actin and γ-actin

(encoded by the *Actb* and *Actg1* genes, respectively) and four muscle-specific isoforms: α-skeletal actin, α-cardiac actin, α-SMA, and γ-enteric smooth muscle actin, which are translated from the *Acta1*, *Actc1*, *Acta2*, and *Actg2* genes (26).

The various actin isoforms differ in their N-terminal regions, which influences their ability to activate myosin motors (27). These isoforms have conserved patterns, whereas myosins are variable depending on their functionality (28). In mammals, 40 different myosin genes may be expressed (29). Myosins consist of heavy (MHC) and light chains (MLC) (29). Calcium-dependent phosphorylation of MLC by MLC kinase induces contraction in smooth muscle cells (30). Like smooth muscle cells, pericytes also contract depending on intracellular calcium concentration. Electrical stimulation of pericytes evoked constriction, while removing the extracellular calcium induced dilation (24).

According to database analyses based on single-cell RNA sequencing (31,32), among the genes encoding MHCs, *Myh11* and *Myh9* are expressed by pericytes; however, this latter is not specific to these cells. Among genes encoding MLCs, *Myl9* is the most abundant and specific to vascular smooth muscle cells (VSMCs) and pericytes in the brain. These online tools confirmed that the *Actb* gene is highly expressed in the cells classified as pericytes, while only small amounts of *Acta2* and *Actg1* was detected. On the protein level, the expression of β-actin in pericytes of the central nervous system (CNS) is well-established and unquestioned; however, the expression of α-SMA and γ-actin has been a subject of debate.

Mid-capillary pericytes in tissue sections (12) or *in vivo* (13) were reported not to express α-SMA, but to express Myh11 protein; while ensheathing pericytes were shown to express both (33). However, strategies which allow for F-actin fixation uncovered the presence of α-SMA in high-order pericytes as well. It has been shown that the low level of α-SMA expressed in capillary pericytes suffers rapid depolymerisation upon classical tissue handling procedures, and the resulting dispersed fibres are difficult to detect (34). Additionally, pericytes exhibit high expression of myosin 1b, which is an actin depolymerase (35), potentially responsible for the rapid depolymerisation of α-SMA in these cells. Another explanation for the low levels of α-SMA in capillary pericytes might be that a different isoform of actin is involved in the contraction. Although, γ-SMA is less abundant in vascular tissues, it has been showed that it might be expressed by pericytes (36). Since γ-SMA appears to be the most dynamically remodelled actin isoform within VSMCs (37), it may play a critical role in the regulation of mural cell contractility.

Nevertheless, the small amounts of α-SMA may be sufficient to mediate the contraction of capillary pericytes via the actomyosin complex, and this could also explain the slower kinetics of diameter changes in high order capillaries of the brain.

Earlier studies demonstrated that TGF-β regulates the expression of α-SMA in pericytes (38), fibroblasts (39), and aortic smooth muscle cells (40). Furthermore, TGF-β was found to be important in the regulation of vascular tone because it may suppress the production of vasodilators (such as nitric oxide) and promote the production of vasoconstrictors (such as endothelin-1) (41). These vasoactive mediators have effects on ensheathing and capillary pericytes (23); therefore, TGF-β may act on the contractility of pericytes indirectly as well.

Taken together, expression of α-SMA of pericytes may be crucial for regulation of CBF. On the other hand, pathological conditions as well as ageing could lead to dysregulation of contractile properties of pericytes and impaired neurovascular coupling.

3. Changes in the brain during ageing

a. Age-related microvascular changes

Ageing has a strong impact on the brain microvasculature in regards of morphology and function as well. Age-related morphological changes include vessel rarefaction, fibrosis, basement membrane thickening, and microhaemorrhages (42,43). Furthermore, ageing is associated with alteration in regulation of cerebral circulation (44) and in BBB permeability (45,46).

Among the morphological alterations, the most conspicuous is the change in number of vessels. Normal ageing leads to reduction in vascular length and branching density (47) and increase of vessel tortuosity across all brain regions (47,48). The ultrastructure of cellular and acellular components of the BBB also alters, which may be associated with functional impairments. Loss of tight junction proteins in endothelial cells has been suggested to be the main reason for increased capillary permeability and enhanced delivery of neuroinflammatory molecules in aged brains (49). The thickness of the basement membrane may double in ageing through lipid accumulation (50) and collagen deposits (51), which indicate impaired lipid and protein metabolism. Brain imaging studies showed that the prevalence of microbleeds increases gradually with age (52), and age-related microbleeds highly depend on systemic inflammation (53). During ageing, a low-grade systemic inflammation develops, called inflamm-ageing (54), which contributes significantly to age-related pathologies. Inflamm-ageing greatly affects the cells of the BBB as well. Change of the gene expression profile to a pro-inflammatory one has

been described in brain endothelial cells and glial cells resulting in the development of neurodegeneration (55).

b. Age-related changes in brain pericytes

Brain pericytes play a crucial role in BBB integrity and CBF, and age-related changes highly affect these functions.

Ageing contributes to reduction in number of pericytes in the frontal cortex, mainly in Brodmann area 9 (56), the basal forebrain, and the deep cortical layers (47). Focal loss of pericytes causes vasodilation, which results in increased flow heterogeneity in capillary networks (57). Watson *et al.* showed that while the number of pericytes decreased, pericyte coverage remained unaffected (58), which suggests that pericytes try to fill the gaps by remodelling their processes (59). However, in the ageing brain, pericyte remodelling is slower which leads to persistent focal vasodilations and disrupted capillary flow and structure (57). Some researchers have shown that not only the number, but also the coverage of pericytes decreases, and that these changes are associated with reduced CBF in the cortex and hippocampus (60,61). Additionally, 20% loss of pericyte coverage initiated BBB disruption and microvascular reduction, while greater, 40% loss resulted even in neuronal damage (60). The link between pericyte loss and neurodegeneration can also be explained by the fact that pericytes express pleiotrophin, a neurotrophic growth factor that maintains neuronal health (61).

Not exclusively the pericyte loss, but the damage of pericytes is also pronounced in higher age, and this is related to BBB disruption and neuroinflammation (62). Cai *et al.* did not find change in number of mural cell soma during ageing, but observed a reduction of pericytes' processes. Additionally, vessel diameter increased, reducing vascular resistance, while vascular responsivity decreased, contributing to the reduction in neurovascular coupling responses in old mice (63).

4. Microinfarcts in the ageing brain

a. Causes and consequences of cerebral microinfarcts

Cerebral microinfarcts are small lesions of cellular death or tissue necrosis, which have presumably ischaemic origins. Because of their small size (0.2–2.9 mm) microinfarcts typically remain undetected by classical brain imaging; however, microscopy studies revealed substantial amounts of microinfarcts in the brains of the elderly persons (64). Although they are invisible to the naked eye, the causes and consequences related to them are evident.

As mentioned in the previous chapter, ageing contributes significantly to microvascular changes. These changes can lead to cerebral small vessel disease, hypoperfusion, and microemboli which are the main causes of cerebral microinfarcts (65). Cerebral amyloid angiopathy and arteriolosclerosis, two types of cerebral small vessel disease often coexist with microinfarcts (66). In severe amyloid angiopathy, higher burden of microinfarcts were observed compared to the mild form of the disease (67). In watershed zones, which are located at the junction of two vascular territories, hypoperfusion seems the most important factor in the development of microinfarcts (68). Reduced CBF was also found to induce cerebral microinfarcts in memory clinic patients (69) and in patients with Alzheimer's disease (AD) (70). Microinfarcts are usually caused by microemboli in patients with atherosclerosis or heart disease (71). To study microinfarcts, most of the animal studies use the strategy based on the pathomechanism of microembli to induce microinfarcts, like intra-arterial injection of microbeads (72) or cholesterol crystals (73).

Cerebral microinfarcts are associated with several ageing-related pathologies. Larger number of cortical microinfarcts increase the risk of cognitive decline and dementia (74–76), while subcortical ones are related to impaired mobility (76) or depression (77). Moreover, it has been suggested that tiny acute infarcts can cause leukoaraiosis, a white matter abnormality (78), and vascular cognitive impairment (69).

b. The role of brain pericytes in microinfarcts

Ischaemic injury is strongly correlated with pericyte dysfunction. Brain pericytes show high responsivity to cerebral microinfarcts, and pericyte dysfunction increases the risk of ischaemia (79,80).

Although pericytes help to regulate capillary blood flow through their contractile function, this mechanism can become harmful in the context of ischaemia. It has been described that chemical ischaemia (medium and high doses of iodoacetate and antimycin-A) induces pericyte contraction *in vitro* (81). *Ex vivo* studies of cerebral cortical slices revealed that pericytes constricted capillaries in response to ischaemia in an oxygen-glucose deprivation model (20). In intact mouse brain ischaemia induced by middle cerebral artery occlusion, contraction of pericytes was observed, and pericytes remained contracted despite of reopening of the occluded artery, causing capillary constriction (82). This is called the no-reflow phenomenon, which was first observed by Majno *et al.* (83) and described in more detail by Ames *et al.* in rabbit brains (84). In the clinics, despite the successful clot removal of stroke

patients via thrombectomy or thrombolysis, failure of reperfusion can occur because of the no-reflow phenomenon, worsening the clinical outcomes (85).

During ischaemic events, BBB disruption may also enhance neuronal injury, to which the contribution of pericytes is noteworthy. Activation of matrix metalloproteinase-9 in pericyte somata leads to BBB damage and plasma leakage (86). Additionally, increased BBB permeability was found to be the consequence of the expression of pericyte-derived vascular endothelial growth factor during stroke (87).

5. Other pathologies that induce vasoconstriction

In addition to microinfarcts, brain metastatic tumours lodged in cerebral capillaries can also induce vasoconstriction and even vessel obstruction (88), suggesting the potentially important role of pericytes in these processes.

Brain metastases are secondary tumours spreading to the CNS from a primary tumour through the bloodstream (89). They originate most commonly from lung cancer, breast cancer and melanoma (90). To enter the brain, tumour cells have to cross the BBB, which plays a dual role in metastasis formation. While it acts as a physical barrier preventing cancer cells from entering the CNS, it also contributes to supporting metastatic cells during their extravasation and proliferation within the brain (90).

Studies from our laboratory suggest that pericytes have pro-metastatic features in breast cancer by secreting extracellular matrix proteins, such as collagen IV and fibronectin, and growth factors, such as insulin-like growth factor 2 (91). Additionally, it has been shown that mammary carcinoma cells induce vasoconstriction following 24–48 hours of residence within the lumen of parenchymal vessels (88), in which pericytes may have an important role. In glioblastoma, α-SMA expressing pericytes exhibit abnormal proliferation, which contributes to the tumour-associated vascular malformations (92). Furthermore, GBM cell–pericyte fusion hybrids have been observed on abnormally constricted vessels located ahead of the tumour, where they appear to contribute to hypoxia that promotes tumour progression (93).

Based on these data, pericytes appear to play a significant role in vascular changes in response to tumour cells. However, the contractile proteins underlying these mechanisms remain unidentified.

V. Aims of the study

Pericytes are key regulators of the cerebral microcirculation through their contractile properties. However, in ageing and in ageing-associated diseases several microvascular changes occur including microinfarcts, which may alter the functions of pericytes as well. In this study, we aimed to understand how ageing, microinfarcts, and metastatic cells influence the expression of contractile elements of pericytes, and how these changes potentially cause CBF disturbances. Our research focused on four main questions:

1. First, how does the expression of α-SMA change during ageing in pericytes, and what is the regulator of the α-SMA change?
2. Second, do microinfarcts induce changes in the expression of α-SMA of pericytes in young and old mouse brains?
3. Third, do other contractile proteins, like γ-actin play a role in the contractility of pericytes in the context of ischaemia?
4. Finally, do metastatic tumour cells induce the expression of α-SMA in cerebral pericytes?

VI. Materials and methods

1. Animals

All mice were housed and treated in accordance with the Directive 2010/63/EU of the European Parliament on the protection of animals used for scientific purpose, and the protocols were approved by the institutional care and the Regional Animal Health and Food Control Station of Csongrád-Csanád County (permit numbers: XVI./767/2018 and XVI./2161/2024). Altogether, 26 young (2 to 3 months of age) and 21 old (24 months of age) BALB/c mice (Charles River Laboratories, Wilmington, MA, USA), 2 young female (2 to 3 months of age) FVB/Ant:TgCAG-yfp mice, 2 young (2–3 months) and 2 aged (14–21 months) male Wistar rats (ToxiCoop, Budapest, Hungary; received from Franciska Erdő, Pázmány Péter Catholic University, Budapest, Hungary) were used in the study.

2. Microvessel isolation

Young and old mice and rats were anaesthetized with Avertin (a mixture of 2,2,2-tribromoethanol, 2-methyl-2-butanol, and ethanol dissolved in 0.9% NaCl solution) and transcardially perfused with phosphate buffered saline (PBS; 0.1 M, pH = 7.4) to remove blood from the vessels. Brains were taken out and the meninges were removed on Whatman-paper. The brain tissues were homogenized in Dulbecco's modified Eagle's medium/Nutrient Mixture F-12 (DMEM/F-12; Thermo Fisher Scientific, Waltham, MA, USA), then digested with collagenase II (Merck-Sigma, St. Louis, MO, USA) and DNase (Merck-Sigma) for 30 min, at 37°C, and 250 rpm shaking. Samples were diluted with DMEM/F12 and centrifuged at 1000 × *g* for 8 min at 4°C. The pellets were resuspended in 20% bovine serum albumin (BSA) (VWR International, Radnor, PA, USA) and centrifuged at 1000 × *g* for 20 min at 4°C. The resulting pellets were gently mixed in DMEM/F12, and filtered through a 70 μm pore size cell strainer (Corning, Corning, NY, USA), followed by centrifugation at 700 × *g* for 5 min at 4°C. The pellets were resuspended in PBS, and the quality of the microvessels was checked under microscope. Finally, the samples were centrifuged at 600 × *g* for 5 min at 4°C. The final pellets were suspended in TRI Reagent (Thermo Fisher Scientific; for RNA isolation) or radioimmunoprecipitation assay (RIPA) buffer (for western blot). For immunofluorescence, the microvessel fraction was fixed in 4% paraformaldehyde (PFA). The protocol is depicted in Figure 3.

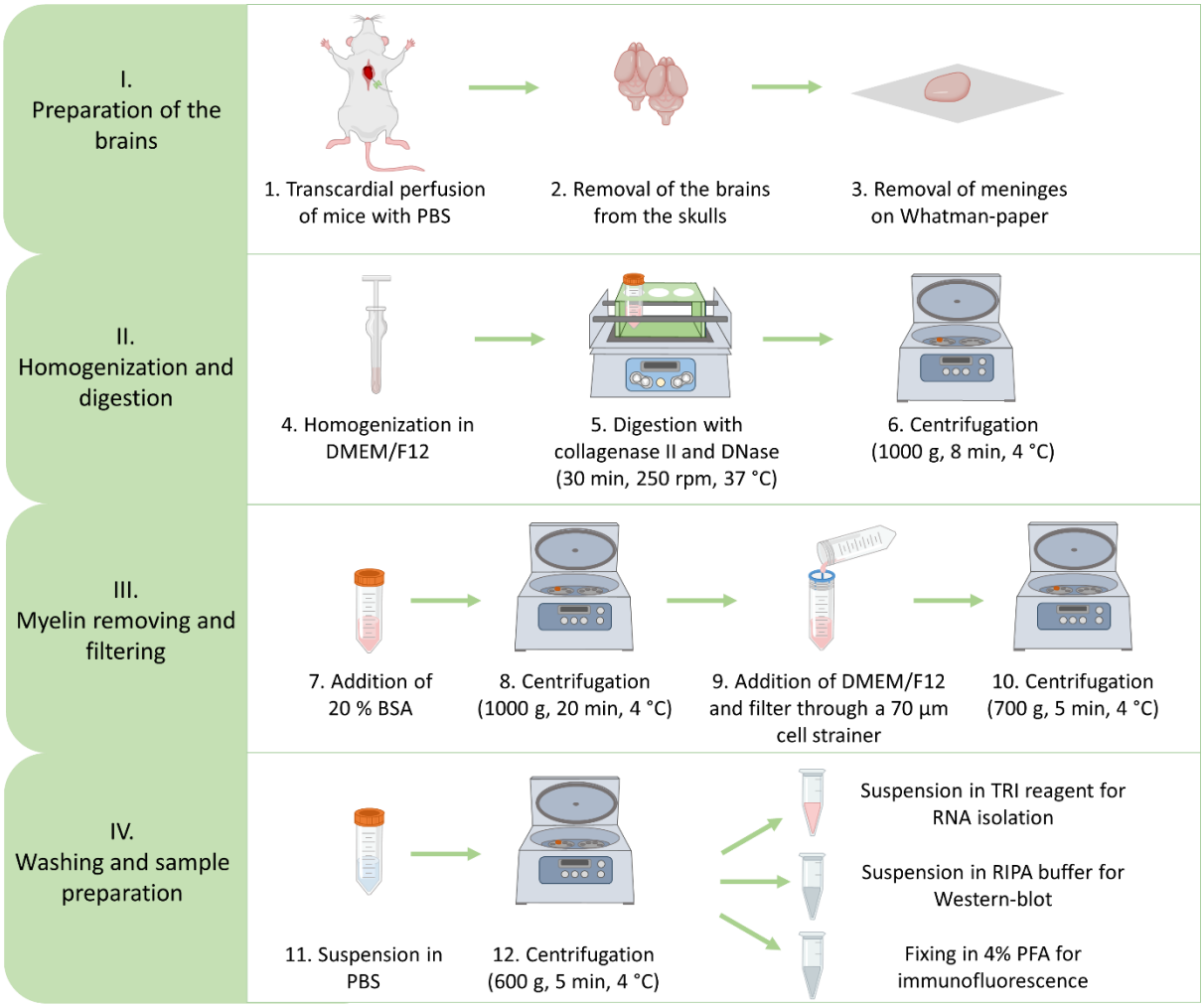

Figure 3. Steps of microvessel isolation from the mouse brain.
The image depicts the steps involved in isolating microvessels from the mouse brain following transcardial perfusion. This protocol utilizes mechanical and enzymatic separation to extract microvessels from brain tissue.

3. RNA isolation and real-time polymerase chain reaction

Total RNA was isolated using Ambion RNAqueous®-Micro Kit (Thermo Fisher Scientific). For reverse transcription, the Maxima First Strand cDNA Synthesis Kit (Thermo Fisher Scientific) was used. Amplification was performed using the iTaqTM Universal SYBR Green Supermix (Bio-Rad, Hercules, CA, USA) on a Bio-Rad iQ5 instrument using mouse *Acta2* (fw: GAGCGTGGCTATTCCTTCGTG; rv: CAGTGGCCATCTCATTTTCAAAGT), *Tgfb1* (fw: CACCGGAGTTGTGCGGCAGT; rv: TGCCGCACGCAGCAGTTCTT), and GAPDH (fw: GGTCTTCCTCGAAGCACTT; rv: GTGAAGACGCCAGTAGACTC) primers under the following conditions: 40 cycles of 95°C for 15 s, 62°C for 30 s, 72°C for 30 s.

4. Western blot

Microvessel samples collected in RIPA buffer were centrifuged at 16,000 × *g* for 15 min at 4°C. Supernatants were collected and protein concentration was determined by the bicinchoninic acid assay (Thermo Fisher Scientific). After addition of Laemmli buffer, the samples were incubated at 95°C for 5 min. Samples were electrophoresed using standard denaturing SDS/PAGE and blotted on polyvinylidene difluoride membranes (0.2 μm pore size; Bio-Rad). After blocking with 3% BSA or 5% nonfat milk in Tris-buffered saline containing 0.1% Tween-20 (TBS-T), membranes were incubated with primary antibodies overnight at 4°C, as follows: anti-α-SMA (Abcam, Cambridge, UK; cat. no. ab5694) in a dilution of 1:2000, anti-TGF-β1 (Santa Cruz Biotechnology, Dallas, TX, USA; cat. no. sc-130348) in a dilution of 1:500, anti-γ-actin (Abcam; cat. no. ab123034) in a dilution of 1:1000, and anti-β-actin (Merck-Sigma; cat. no. A5441) in a dilution of 1:10,000. Blots were washed in TBS-T three times for 10 min, incubated for 1 hour in horseradish peroxidase-conjugated anti-rabbit IgG or anti-mouse IgG secondary antibodies (Jackson Immunoresearch, Cambridgeshire, UK) diluted to 1:3000 in TBS-T, and then washed again in TBS-T. Immunoreaction was visualized with the Clarity Chemiluminescence Substrate (Bio-Rad) in a ChemiDoc MP System (Bio-Rad). Densitometry analysis was performed with the IMAGE LAB Software, version 6.0.0 (Bio-Rad).

5. Surgeries

a. Microocclusion model

Mice were anaesthetized via inhaled isoflurane 4% (v/v) in oxygen for induction and 1-2% (v/v) for maintenance, from a precision vaporizer (Open Circuit Isoflurane Tabletop System, Stoelting, Dublin, Ireland). Depth of anaesthesia was monitored by the toe-pinch test. The surgical procedure is depicted in Figure 4. After dissection of the connective tissue and retraction of the muscles, the right common carotid artery (CCA) was carefully isolated from the tissue. The external carotid artery (ECA) was temporarily ligated with surgical thread. A temporary loop was placed on the proximal section of the CCA, and a sterile cotton ball was placed under the distal section to lift it. A 30G needle was inserted into the artery to inject 100 μl of PBS containing ~4000 Fluoresbrite® YG microspheres (10 μm; Polysciences, Warrington, PA, USA). In control animals, 100 μl of PBS was injected into the circulation. After the injection, bleeding was controlled using hemostatic sponge and sterile cotton swabs, and the loops were removed to restore circulation. After 2, 4 or 24 hours, mice were anaesthetized and

transcardially perfused with PBS, flowed by 100% methanol (MeOH) for actin stabilization, and finally 4% PFA. The brains were removed and post-fixed with PFA at 4°C overnight. On the next day, the brains were placed into 30% sucrose solution in 0.1 M PBS, and stored at 4°C until sectioning.

For microvessel isolation, mice received ~250,000 Fluoresbrite® YG microspheres in the right internal carotid artery (ICA). After 4 hours, microvessels were isolated as described previously separately from the two hemispheres and collected in RIPA buffer.

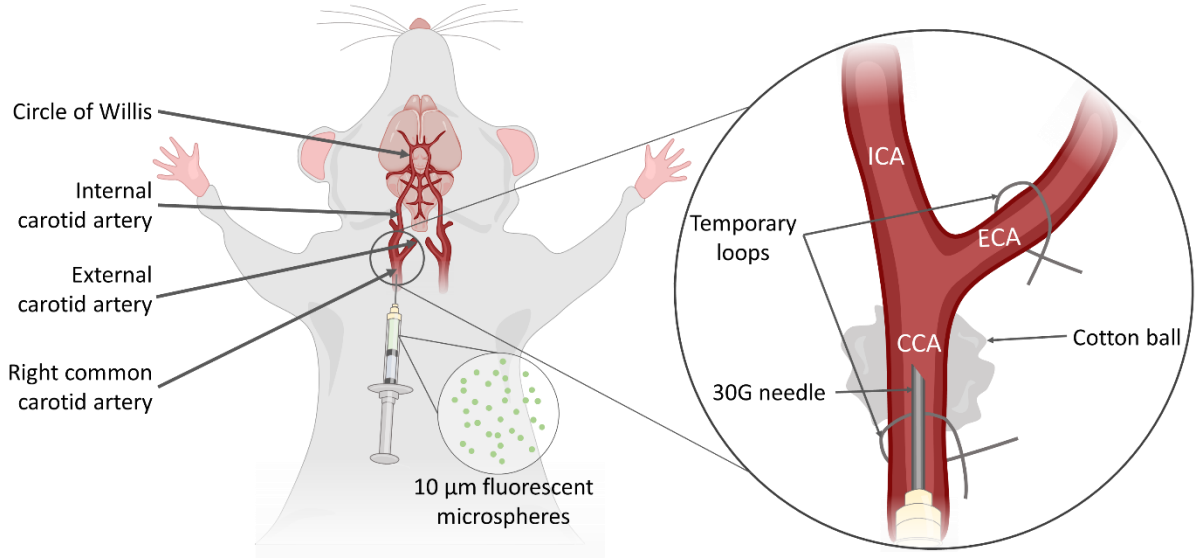

Figure 4. Microsphere injection through the carotid artery in mice.
Schematic representation of the mouse cerebral vascular system, including an illustration of the common carotid artery (CCA) branching into the internal carotid artery (ICA) and the external carotid artery (ECA). The CCA and ECA were temporarily ligated prior to the injection. Fluorescent microspheres diluted in PBS were injected into the brain circulation through the CCA using a 30G needle.

b. Microinjection and sample preparation

To block F-actin depolymerization in vivo, stereotaxic injections of jasplakinolide (10 µM in PBS- dimethyl sulfoxide; Tocris, Bio-Techne; cat. no. 2792) combined with 0.05% fluorescein-dextran (70 kDa; Merck-Sigma) to see injection tracks, was performed unilaterally at four sites into the parietal cortex of mice. Injection was carried out using a glass micropipette (Drummond Scientific Company, Broomall, PA, USA) with a long narrow tip (~20 µm) pulled with a micropipette puller (Sutter Instrument, Novato, CA, USA). The micropipette was inserted into the brain through a burr hole of 1–1.5 mm diameter and jasplakinolide was infused at a flow rate of 6 nl/seconds at depths of 200 µm, 300 µm, 400 µm, 500 µm and 600 µm (100 nl per injection location) with a programmable nanoliter injector (Nanoject III, Drummond Scientific Company). Two hours after intracerebral injection, in order to have a quick fixation

to avoid actin depolymerization, brains were collected after decapitation and 2 mm-thick pieces of tissue containing the injection sites were immediately cut out in brain matrix soaked in ice-cold PBS. To preserve antigenicity of actin (94), tissues were immersed in ice-cold Methacarn (MeOH–chloroform–glacial acetic acid 6:3:1) and kept at 4°C for overnight. Methacarn was changed twice with 100% MeOH (for 2 hours and then 3 hours), followed by descending MeOH series (95%, 75%, 50%, 25%), each for two or more hours. Finally, the tissues were transferred to and stored in 0.1 M PBS until sectioning. Sections of 30 or 50 µm were cut on a cryostat (Leica CM1860) and air dried on silane-coated glass microscope slides.

c. Tumour cell injection

Before the procedure, mice were anaesthetized and the CCA was isolated as previously described (see: chapter VI.5.a). FVB/Ant:TgCAG-yfp mice received $1{,}5 \times 10^6$ 4T1-tdTomato cells through intracarotid injection. After 2 days, mice were anaesthetized and transcardially perfused with PBS, followed by 100% MeOH, and 4% PFA. The brains were extracted and post-fixed in PFA overnight at 4°C. The following day, they were transferred to a 30% sucrose solution in 0.1 M PBS and stored at 4°C until sectioning.

6. Immunofluorescence, fluorescence microscopy and quantification of signals

a. Immunofluorescence staining

Isolated microvessels were placed onto adhesive microscope slides. Blocking and permeabilization were performed with PBS containing 3% BSA and 0.5% Triton X-100 (Merck-Sigma) for 1 hour. Primary antibodies were added in the blocking solution in which microvessels were incubated overnight at 4°C. The antibodies were the followings: anti-CD13 (Bio-Techne, Minneapolis, MI, USA; cat. no. AF2335) in a dilution of 1:200, and collagen IV (Abcam; cat no. ab6586) in a dilution of 1:100. After washing in PBS, microvessels were incubated with secondary antibodies diluted to 1:500 in PBS. Anti-goat Alexa Fluor 488 (Thermo Fisher Scientific; cat. no. A32814) and anti-rabbit Alexa Fluor 594 (Thermo Fisher Scientific; cat. no. A32754) were used.

Fixed brains containing microspheres were mounted onto a freezing microtome (Reichert-Jung, Leica, Wetzlar, Germany) and 30 µm-thick coronal sections were cut, which were stored in PBS containing 0.02% sodium azide. Antigen retrieval was performed by incubating the sections in 10 mM sodium citrate (pH = 6) for 10 min at 85°C. All sections were permeabilized in 0.5% Triton X-100 for 30 min, then blocked with 3% BSA in PBS containing

0.3% Triton X-100 for 1 hour. Primary antibodies were diluted in PBS containing 3% BSA and 0.5% Triton X-100, and sections were incubated overnight at 4°C on an orbital shaker. The following antibodies were used: anti-CD13 (Bio-Techne, Minneapolis, MI, USA; cat. no. AF2335) in a dilution of 1:200, and anti-α-SMA (Abcam; cat. no. ab5694) in a dilution of 1:100. Sections were extensively washed in PBS. Anti-goat Alexa Fluor 594 (Thermo Fisher Scientific; cat. no. A-11058), and anti-rabbit STAR RED (Abberior, Göttingen, Germany; cat. no. 2-0012-011-9) were applied as secondary antibodies in a dilution of 1:500 in PBS for 1 hour at room temperature in the dark. Sections were washed, counterstained with a nuclear dye (Hoechst 33342; Merck-Sigma, dilution: 1:1000) for 10 min, washed again with PBS, rinsed in water, and mounted in FluoroMount-G (SouthernBiotech, Birmingham, AL, USA).

For γ-actin staining, sections from brains that had been injected with jasplakinolide were used. The staining was performed as described above. As a primary antibody, anti-γ-actin (Abcam; cat. no. ab123034), and von Willebrand factor (vWF) (Abcam; cat. no. ab6994) were used in a dilution of 1:50, while the secondary antibodies were anti-mouse Alexa Fluor 647 (Thermo Fisher Scientific; cat. no. A32787) and anti-rabbit Alexa Fluor 488 (Thermo Fisher Scientific; cat. no. A32790) diluted to 1:500.

b. Fluorescence microscopy

Samples were analysed using a STEDYCON (Abberior Instruments, Göttingen, Germany) built on an Axio Observer Z1 inverted epifluorescence microscope (Zeiss, Oberkochen, Germany) equipped with an alpha Plan-Apochromat 100×/1.46 oil immersion objective. Confocal *Z*-stack images for statistical analysis were captured at 100× magnification using the same settings for each image.

c. Quantification of the signals

Percentage of α-SMA-positive microvessels blocked by microspheres was calculated by counting the total number of microspheres in 7-12 sections and the number of microspheres localized in α-SMA-positive vessels in the same sections. The ratio was calculated by dividing the microspheres found in α-SMA-positive vessels with the total number of microspheres.

The mean grey values of α-SMA signals were measured using the ImageJ software. The ROIs were selected manually based on the presence of the CD13 signal. The measurements of vessels with lodged microspheres (26 vessel from 2 young, 23 vessels from 2 old mice) were compared to control vessels (69 vessels from 3 young, 82 vessels from 3 old mice).

Additionally, vessels had to meet the criterion of containing CD13-positive pericytes, which were categorized as being ensheathing, mesh or thin-strand based on the morphology. Ensheathing pericytes were recognized as elongated mural cells enwrapping the whole vessel, having a protruding cell body, while mesh pericytes were considered those perivascular cells which incompletely covered the endothelium, frequently localized at branching points.

7. Statistical analysis

Values are expressed as mean ± SEM. Two-group comparisons were performed with Student's *t*-test using the Excel 2016 Data Analysis plugin. Unless otherwise noted, multiple comparisons were evaluated using one-way analysis of variance (ANOVA) and *post hoc* comparisons were assessed by Tukey's multiple comparisons test using GraphPad Prism 8.

VII. Results

1. Age-related changes in the contractile protein expression of brain pericytes

To investigate contractile protein expression in the cerebral microvessels of young and old mice, we first isolated small vessels from the brains of young (2 to 3 months of age) and old (24 months of age) BALB/c mice. Isolated microvessels contained endothelial cells and pericytes (Figure 5 a).

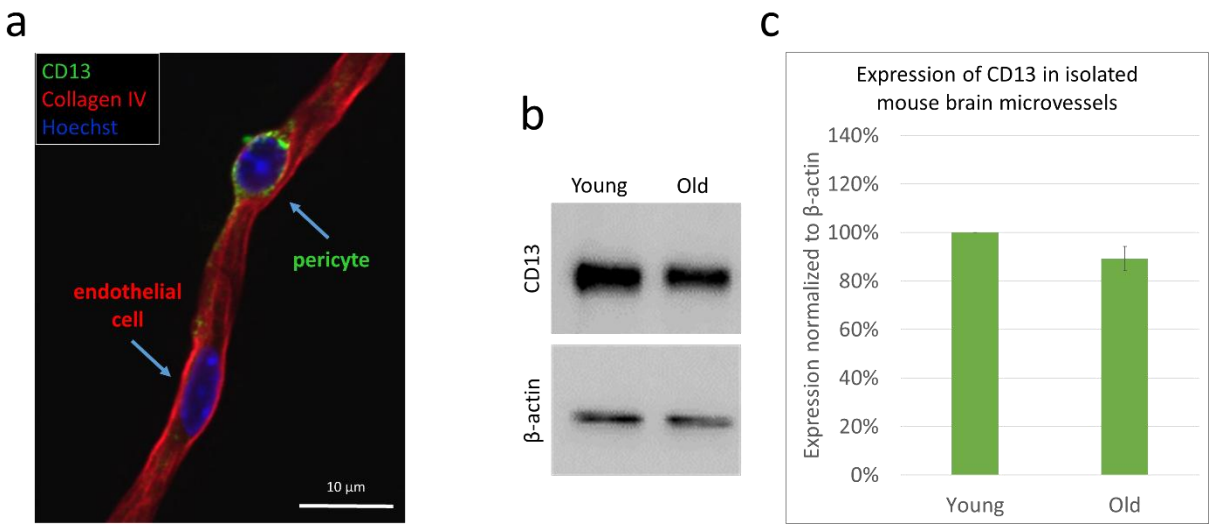

Figure 5. Expression of CD13 in isolated brain microvessels of young and old mice.
a: Representative immunofluorescence micrograph (maximum intensity projection) showing an isolated brain microvessel. **b**: Representative western blot showing the expression of CD13 in brain microvessels of young and old mice (β-actin was used as a loading control). **c**: Quantitative analysis of CD13 levels compared to β-actin expression, as assessed by western blot. Graphs represent the average ± SEM (N = 2). No significant difference was detected between the two groups (Student's *t*-test).

Comparing microvessels of young and old mice, we observed that the amount of CD13 (aminopeptidase N) protein did not change significantly with ageing (Figure 5 b, c). On the other hand, expression of *Acta2*/α-SMA decreased drastically both on the mRNA and protein levels in the microvessels of old mice in comparison to microvessels isolated from the brains of young animals (Figure 6 a-c). Since the decrease in the amount of α-SMA was much more pronounced than that of CD13, this suggests that not change in pericyte number, but rather that of protein expression is responsible for the observed phenomenon.

In both VSMCs and pericytes, one of the main regulators of α-SMA expression is TGF-β1 (95,96). Therefore, we next analysed the expression of *Tgfb1*/TGF-β1 and detected significantly lower gene and protein expression levels in the 2-year-old mice than in the young (Figure 6 d-f). This is in line with the decreased expression of *Acta2*/α-SMA, most probably contributing to this latter.

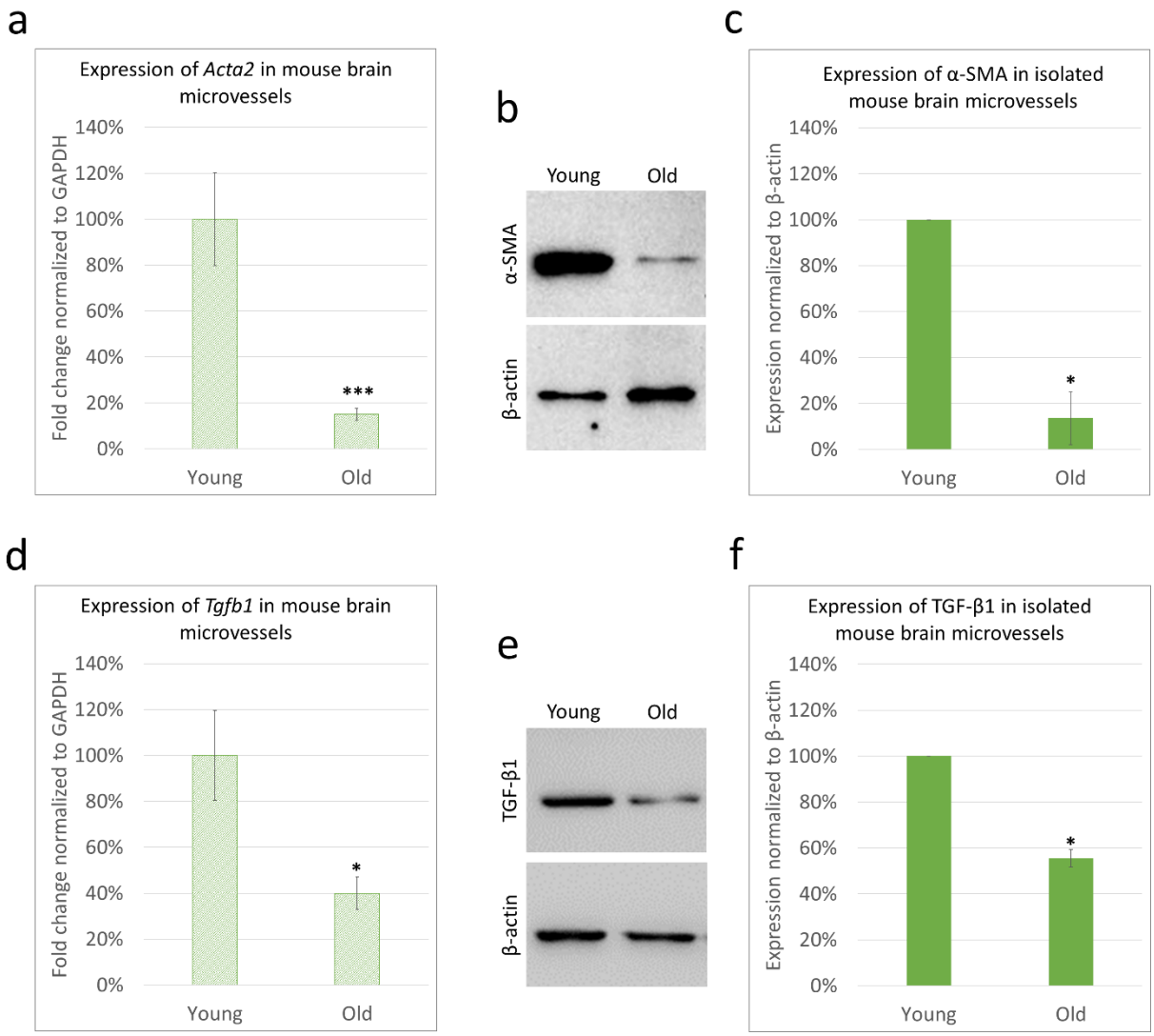

Figure 6. Expression of *Acta2*/α-SMA and *Tgfb1*/TGF-β1 in brain microvessels of young and old mice.

a: Gene expression of *Acta2* in microvessels isolated from the brains of young (2 to 3 months of age) and old (24 months of age) BALB/c mice. Graphs represent the fold change (normalized to GAPDH), average ± SEM (N = 2 independent experiments, each performed in triplicate). *** P≤0.001 (Student's *t*-test). **b**: Representative western blot showing the expression of α-SMA in brain microvessels of young and old mice (β-actin was used as a loading control). **c**: Quantitative analysis of α-SMA levels compared to β-actin expression, as assessed by western blot. Graphs represent the average ± SEM (N = 2). * P≤0.05 (Student's *t*-test). **d**: Gene expression of *Tgfb1* in microvessels isolated from the brains of young (2 to 3 months of age) and old (24 months of age) BALB/c mice. Graphs represent the fold change (normalized to GAPDH), average ± SEM (N = 2 independent experiments, each performed in triplicate). * P≤0.05 (Student's *t*-test). **e**: Representative western blot showing the expression of TGF-β1 in brain microvessels of young and old mice (β-actin was used as a loading control). **f**: Quantitative analysis of TGF-β1 levels compared to β-actin expression, as assessed by western blot. Graphs represent the average ± SEM (N = 2). * P≤0.05 (Student's *t*-test).

Similar results were obtained from young (2–3 months) and old (14–21 months) Wistar rats regarding to the contractile protein amount. *Acta2*/α-SMA expression exhibited a significant downregulation at both transcript and protein levels in cerebral microvessels of aged rats, relative to those isolated from young animals (Figure 7).

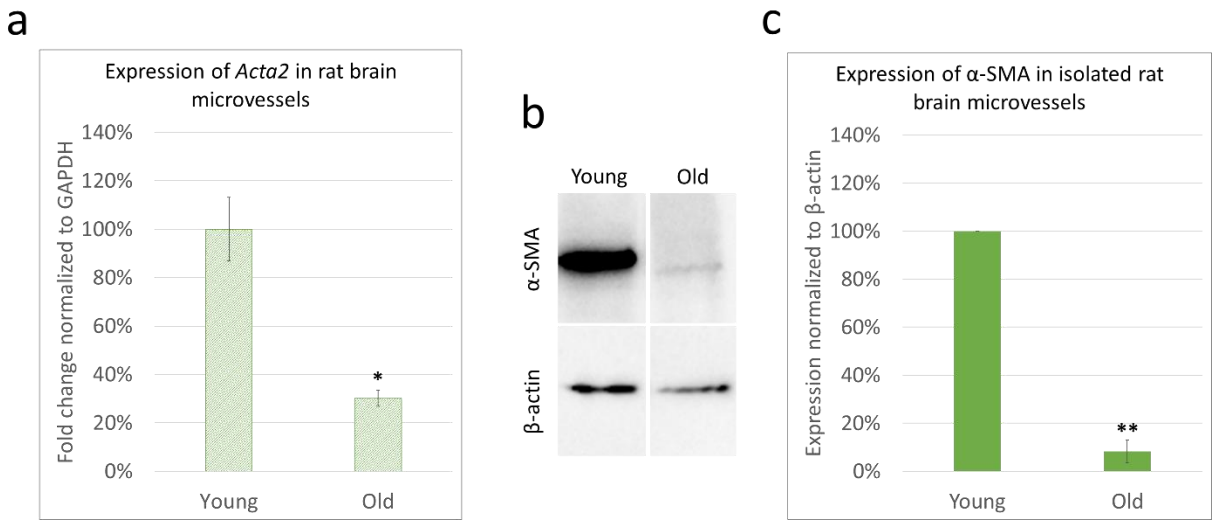

Figure 7. Expression of *Acta2*/α-SMA in brain microvessels of young and old rats.
a: Gene expression of *Acta2* in microvessels isolated from the brains of young (2 to 3 months of age) and old (14–21 months of age) Wistar rats. Graphs represent the fold change (normalized to GAPDH), average ± SEM (N = 2 independent experiments, each performed in triplicate). * P≤0.05 (Student's *t*-test). b: Representative western blot showing the expression of α-SMA in brain microvessels of young and old rats (β-actin was used as a loading control). c: Quantitative analysis of α-SMA levels compared to β-actin expression, as assessed by western blot. Graphs represent the average ± SEM (N = 2). ** P≤0.01 (Student's *t*-test).

2. Changes in α-SMA expression in brain pericytes in response to microsphere-induced lumen obstruction

As cerebral microinfarcts are common in ageing, we next aimed at understanding how contractility of mural cells might influence the outcome of vessel obstruction. We modelled this condition by delivering fluorescent microspheres of 10 μm diameter into the brain vessels of mice via injection into the ICA. In accordance with previous results (72), we observed the highest number of microspheres blocked in the neocortex (in young mice, 33.43%, while in old mice, 32.47% of the total number), followed by the thalamus (15.01% and 13.90%, respectively) and the hippocampus (8.93% in young and 11.63% in old animals) (Figure 8).

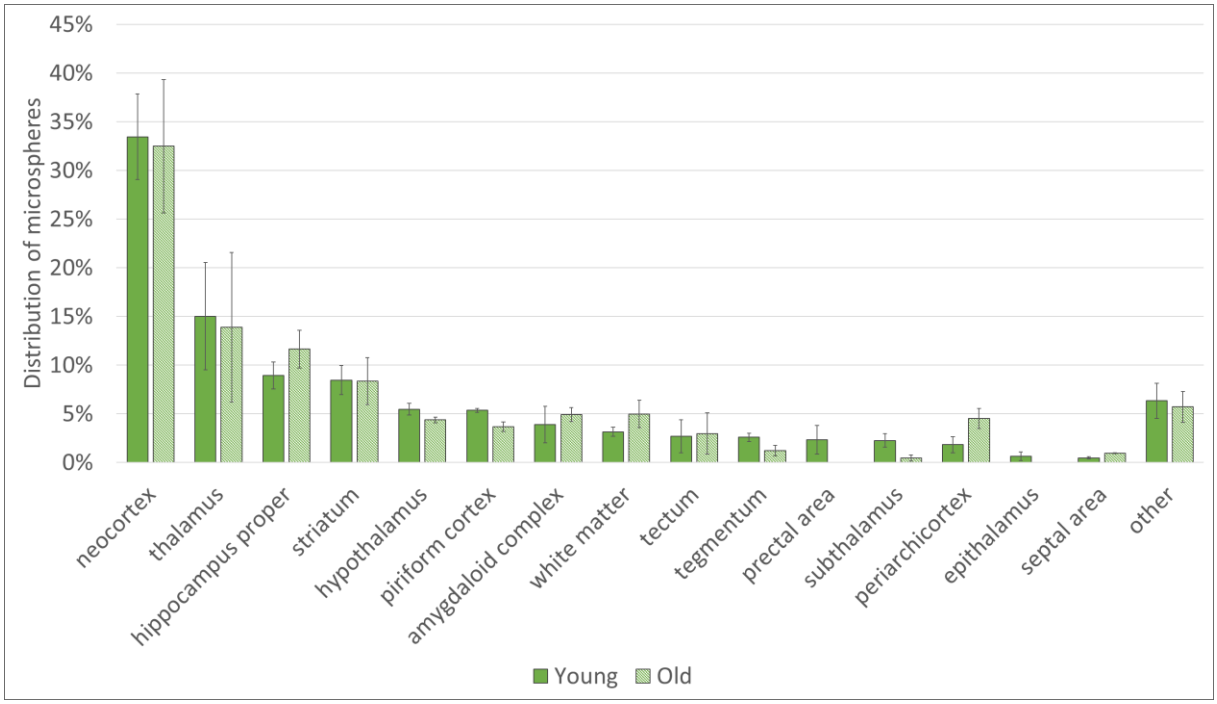

Figure 8. Regional distribution of injected microspheres in the brains of young and old mice. Manual counting shows the distribution of microspheres in the brains of young (2 to 3 months of age) and old (24 months of age) BALB/c mice. Graph represents the percentage of microspheres in each brain region, average ± SEM (N = 2 animals/age group). No significant difference was detected between the two age groups.

Although not significantly higher than at 2 or 24 hours, the number of α-SMA-positive microsphere-containing vessels was the highest 4 hours after injection of the beads, both in young and old animals (Figure 9 a). Therefore, we performed all the subsequent experiments at this time point and focused on evaluating the cortical areas where the majority of the microspheres became lodged. Using immunofluorescence staining of α-SMA in brain sections, we observed a tendency of vasoconstriction in the vessels encompassing the microspheres, although a substantial narrowing of the lumen of blood vessels was a rare event especially in old animals (Figure 9 b).

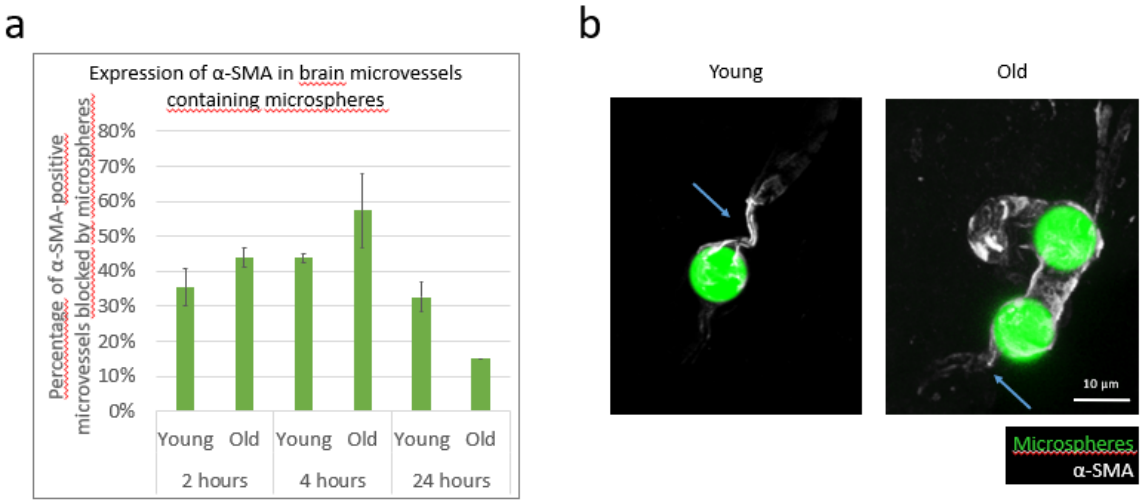

Figure 9. Expression of α-SMA in brain microvessels containing microspheres in young and old mice.
a: Time-dependent expression of α-SMA in microvessels blocked by microspheres, measured by immunofluorescence intensity in young (2 to 3 months of age) and old (24 months of age) BALB/c mice. Graph represents the average ± SEM (n = 7-12 brain sections per animal, N = 2 animals per group). No significant difference was detected among the groups (two-way ANOVA and Sidak's multiple comparisons test). **b**: Representative immunofluorescence micrographs (maximum intensity projection) showing vasoconstriction in the vicinity of the microspheres (indicated by arrows).

We quantified and compared α-SMA expression intensity in the microbead-containing and control hemispheres of young and old mice. As expected, in both age groups, ensheathing pericytes were richer in α-SMA than mesh pericytes. Decreased levels of α-SMA were detected in both ensheathing and mesh pericytes, respectively, in old animals in comparison to their young counterparts (Figure 10). In young mice, expression of α-SMA increased significantly in both ensheathing and mesh pericytes in response to the presence of the microspheres (Figure 10, Figure 11, and Figure 12). In ensheathing pericytes of old animals there was only a tendency of higher α-SMA expression in microbead-containing vessels versus control vessels (Figure 10 and Figure 11), while in mesh pericytes of 24-month-old animals, α-SMA increased significantly surrounding microbead-containing vessels, approximately reaching the level of that measured in young control vessels (Figure 10 and Figure 12). Increased α-SMA expression was predominantly observed on one side of the microsphere; however, due to the thin sections used, we were unable to determine whether this occurred in the upstream or downstream direction. Changes in thin-strand pericytes are not shown since expression of α-SMA was very low in these cells and only detectable in young animals. Microspheres usually stalled in lower order vessels and were very rarely observed in capillaries covered by thin-strand pericytes.

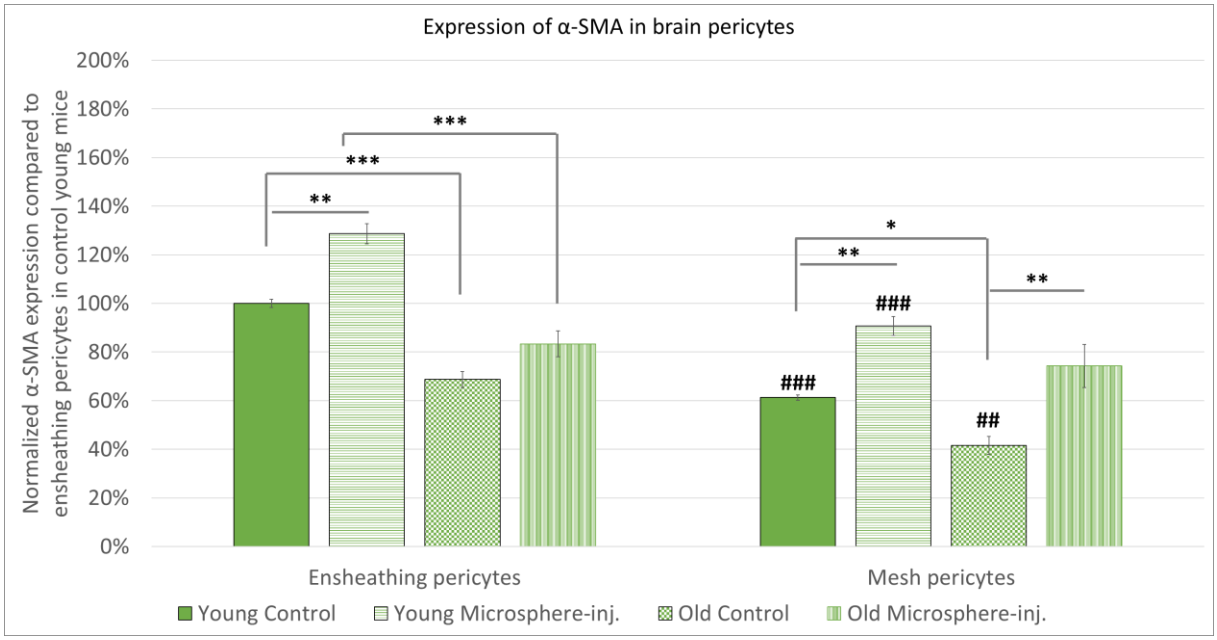

Figure 10. Expression of α-SMA in brain pericytes at 4 hours after injection of microspheres in young and old mice.

Expression of α-SMA in ensheathing and mesh pericytes, measured by immunofluorescence intensity in brain sections of young (2 to 3 months of age) and old (24 months of age) BALB/c mice at 4 hours after injection of the microspheres. Graph represents the average ± SEM (n = 5-10 cells per animal, N = 2 animals per group). * P≤0.05, ** P≤0.01, *** P≤0.001; ## P≤0.01, ### P≤0.001 compared to ensheathing pericytes of the same group (ANOVA and Tukey's multiple comparisons test). Microsphere-inj. = microsphere-injected.

3. Changes in γ-actin expression in brain microvessels following microsphere-induced lumen obstruction

Contractility of pericytes and their involvement in the regulation of CBF has long been debated mainly due to the difficulties in the detection of α-SMA in thin-strand pericytes (97). Contribution of other actin isoforms has been suggested, like γ-actin; however recently, expression of γ-actin was detected only in pericytes of lower order vessels (34). We wanted to acquire a more nuanced understanding of γ-actin expression in brain capillaries and to appreciate whether it shows similar changes as α-SMA in response to lumen obstruction. The same 10 μm-size microbeads were injected unilaterally, but in higher numbers to ensure the majority of microvessels are affected. As detected by western blot, α-SMA increased significantly. On the contrary, expression of γ-actin decreased in microvessels isolated from the microsphere-containing hemispheres (Figure 13 a, b). Finally, we wanted to determine which vascular cells express γ-actin. By performing immunofluorescence staining in isolated microvessels, γ-actin was clearly detected in vWF-positive endothelial cells, but was absent in CD13-positive pericytes (Figure 13 c), suggesting a difference between endothelial cells and pericytes in the expression of actin isoforms both in basal and injured conditions.

Changes in the expression contractile proteins in brain microvascular cells, in response to ageing and microocclusion are summarized in Table 1.

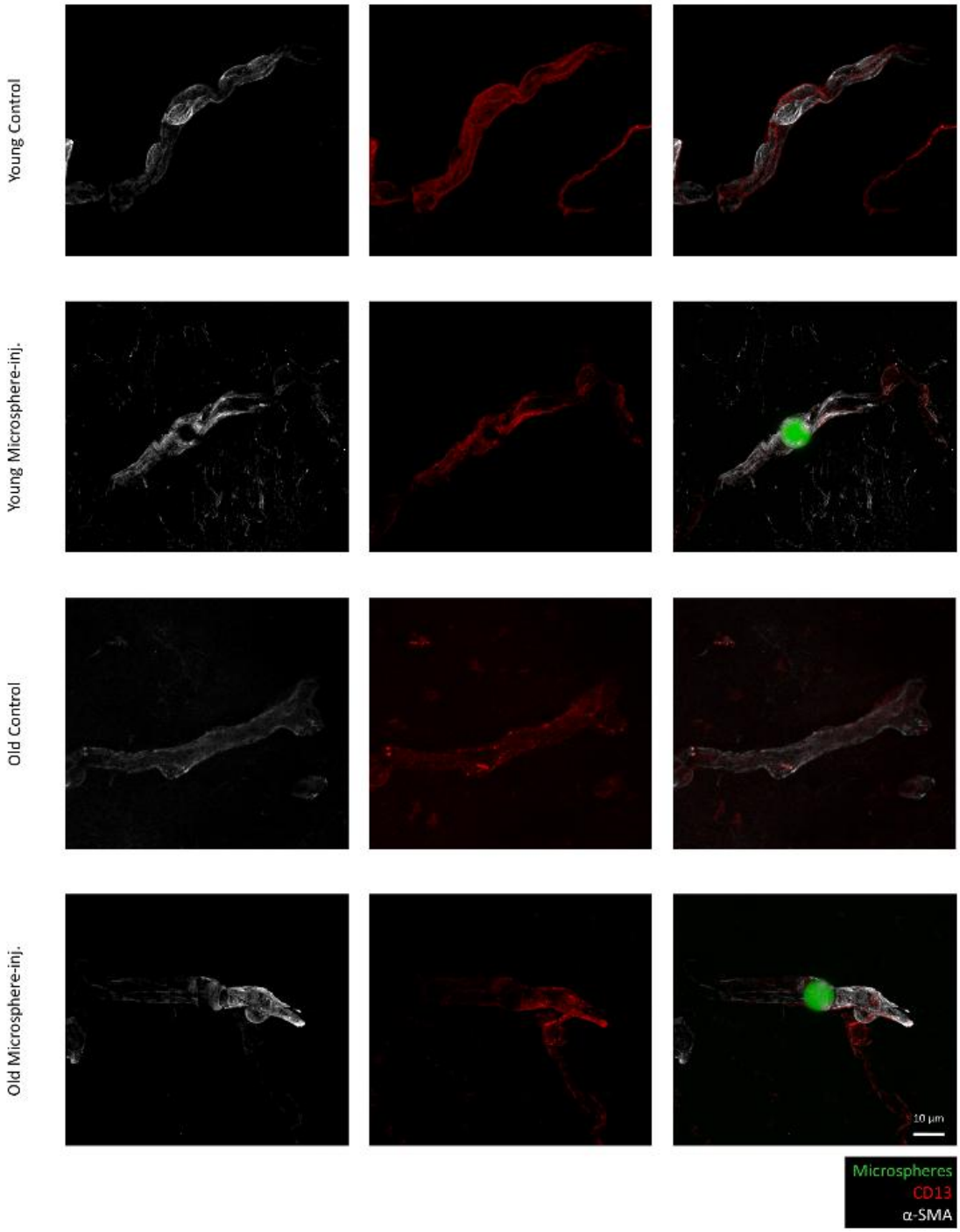

Figure 11. Expression of α-SMA and CD13 in ensheathing pericytes of brain microvessels containing microspheres.
Representative immunofluorescence micrographs (maximum intensity projections) showing α-SMA and CD13 expression in brain sections of young (2 to 3 months of age) and old (24 months of age) BALB/c mice 4 hours after the injection of the microspheres. Microsphere-inj. = microsphere-injected.

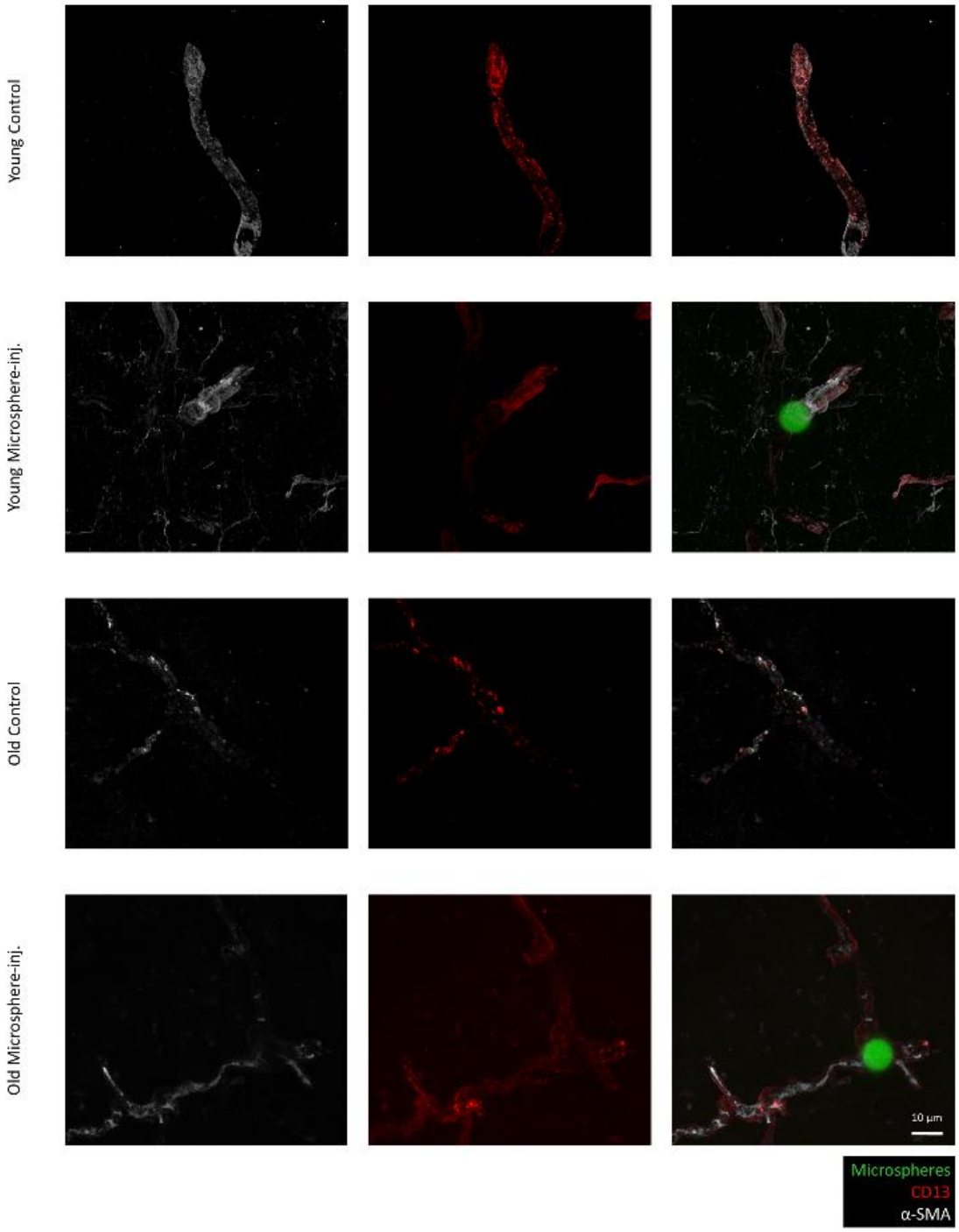

Figure 12. Expression of α-SMA and CD13 in mesh pericytes of brain microvessels containing microspheres.
Representative immunofluorescence micrographs (maximum intensity projections) showing α-SMA and CD13 expression in brain sections of young (2 to 3 months of age) and old (24 months of age) BALB/c mice 4 hours after the injection of the microspheres. Microsphere-inj. = microsphere-injected.

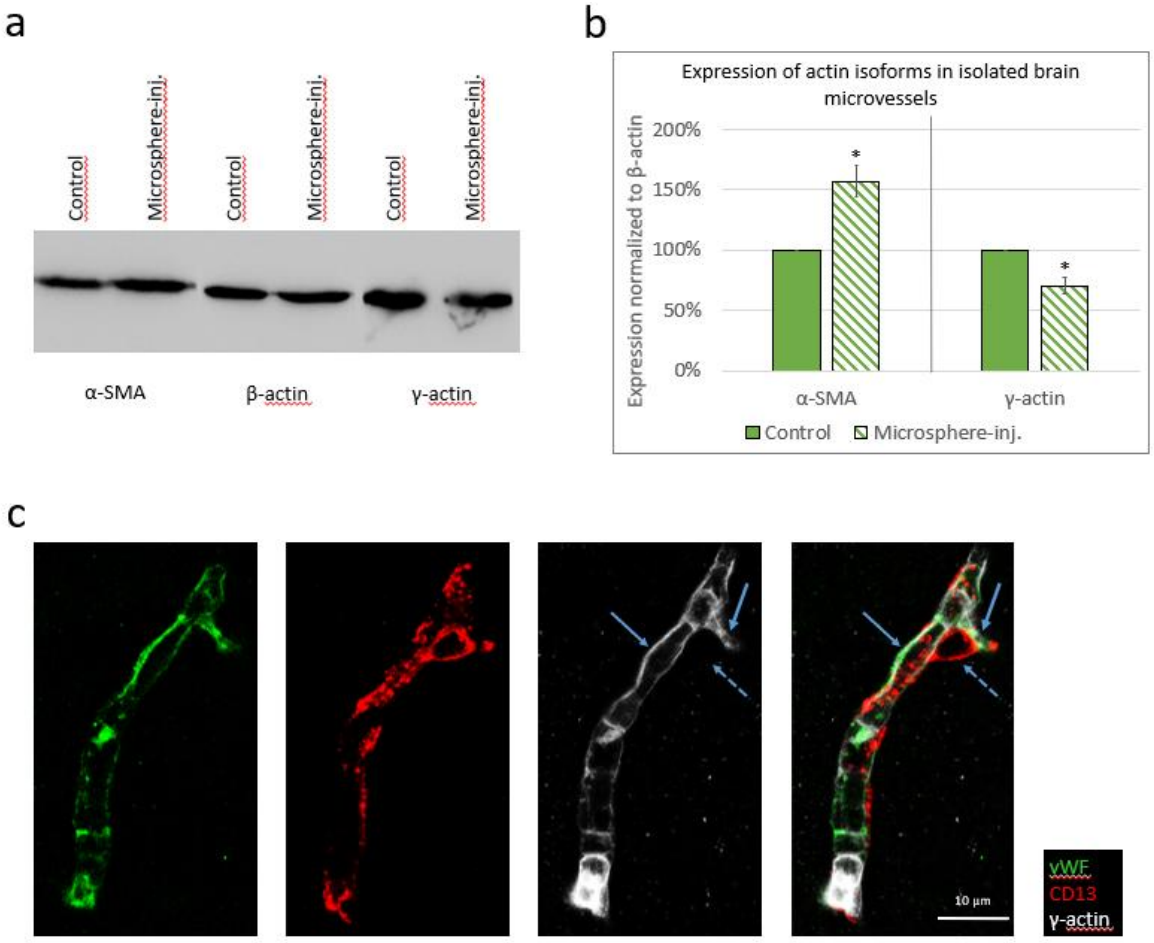

Figure 13. Expression of actin isoforms in brain microvessels.
a: Representative western blot showing the expression of α-SMA, β- and γ-actin in brain microvessels isolated from young mice injected with 10 µm-diameter microspheres. b: Quantitative analysis of α-SMA and γ-actin levels compared to β-actin expression, as assessed by western blot. Graphs represent the average ± SEM (N = 2). * P≤0.05 (Student's *t*-test). c: Representative immunofluorescence micrographs (maximum intensity projections) showing expression of γ-actin in brain sections of young BALB/c mice. Arrows denote endothelial localization of γ-actin. The dashed arrow indicates absence of γ-actin from pericytes.

cerebrovascular cell type	contractile protein	ageing	microocclusion
pericyte (mesh, ensheathing)	α-SMA	↓↓↓	↑↑
microvascular endothelial	γ-actin	?	↓

Table 1. Changes in the expression contractile proteins in brain microvascular cells, in response to ageing and microocclusion.

4. α-SMA expression in brain pericytes in response to tumour cells

It has been previously described in our laboratory that breast cancer cells induce vasoconstriction in the brain after spending 1–4 days in the vessel lumen (88). To elucidate the molecular background of this mechanism, we aimed to investigate the contractile protein expression of pericytes near to the tumour cells. In brain sections of young FVB/Ant:TgCAG-YFP mice, which express Venus yellow fluorescent protein (YFP) in endothelial cells, we observed increased α-SMA expression around cancer cells lodged in microvessels, three days after their injection (Figure 14).

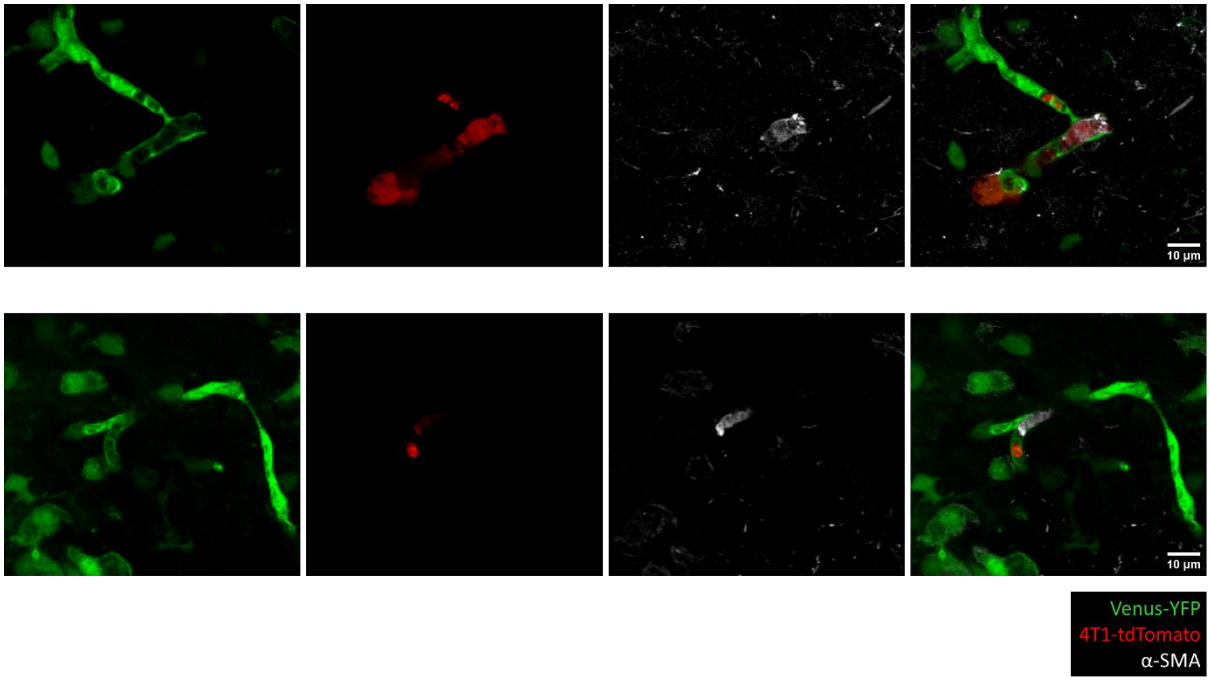

Figure 14. Expression of α-SMA in brain microvessels containing tumour cells.
Representative immunofluorescence micrographs (maximum intensity projections) showing α-SMA expression in brain sections of young (2 to 3 months of age) FVB/Ant:TgCAG-yfp mice (expressing the Venus-YFP in endothelial cells) 3 days after the injection of 4T1-tdTomato cells.

VIII. Discussion

Proper neuronal function relies on a tightly regulated microcirculation that meets the high and continuous metabolic demands of the brain. VSMCs, precapillary sphincters and ensheathing pericytes take a robust activity in regulating vasoconstriction and vasodilation, while capillary pericytes rather participate in the modulation of the effect.

Ageing and ageing-related diseases alter the structure of the cerebral microvasculature, which exacerbates BBB leakage and leads to impaired CBF, as well as a decrease in neurovascular coupling (44,98,99). However, the involvement of pericytes in these processes is far from being completely elucidated.

Here we observed that α-SMA and *Acta2*, the gene encoding it, decrease during ageing in microvessels isolated from mouse brains. Since CD13 did not show a similar change, we conclude that loss of α-SMA is due to a decreased α-SMA content and not a reduction in the density of the pericytes. Moreover, we have also detected a significant drop in vascular α-SMA expression in brain sections, which affected both ensheathing and mesh pericytes.

Previous studies on ageing-related changes in pericytic α-SMA expression and pericyte number are uncertain. In human post-mortem brains, a reduction in pericyte number was observed in the frontal cortex in normal ageing but not in vascular dementias and AD, while other studies described pericyte degeneration in AD (100) and in cognitive impairment (101). Reduction of pericytes may be associated with the deficiency of Notch3 signalling (102,103), which markedly declines in ageing (104). Notch3 loss is further related to dysregulation of calcium and contractile functions in mural cells (104). Moreover, a decrease in the α-SMA content of VSMCs was observed in ageing and especially in AD (105,106).

In mouse models of ageing, pericyte vulnerability and decreased remodelling were shown to result in BBB opening or deficits in CBF (57,58,107). Recently, ageing was proven to decrease vascular responsivity, especially the relaxation ability of precapillary sphincters and of ensheathing pericytes in the mouse brain. This was accompanied by loss of processes, but not of the number or the α-SMA content of mural cells (63).

Although these results are somewhat controversial, several of them point to the reduction in the amount of α-SMA in mural cells, expressly in those with higher contractile protein content, *i.e.* VSMCs and ensheathing pericytes.

On the functional level, ageing-associated changes suggest a contractility decrease in brain vessels. Ageing often causes a decline in CBF, leading to chronic cerebral hypoperfusion. Age-related dementias associated with hypoperfusion accomplish capillary dilation in white

matter, suggesting a compensatory mechanism (108). Additionally, older individuals may show a reduced ability to constrict blood vessels in response to stimuli like hypocapnia (low carbon dioxide), which can indirectly lead to increased vasodilation (109). These observations could point to a downregulation of contractile proteins in mural cells.

In our study, ageing-dependent decline in α-SMA expression of pericytes is further supported by the decreased expression of TGF-β1, which is the main stimulator of α-SMA transcription (40). As previously shown, TGF-β1 induces growth arrest and a contractile phenotype in pericytes through Myf-5- and Smad2-mediated signalling (110). Among cells of the BBB, both endothelial cells and pericytes, as well as astrocytes secrete TGF-β1 (111–113), having diverse effects on endothelial cells (112–115) and pericytes. As a limitation of our study, we have not tested which cell types downregulate TGF-β1 expression in the brain microvessels of old mice. In addition, it has to be noted that TGF-β signalling has diverse effects in cerebral ageing (116).

Ageing is a risk factor for brain ischaemic lesions as well, among which microinfarcts are very common. These are microscopic lesions with a wide distribution in the brain, affecting a large number of vessels (117). Brain microinfarcts are often correlated with small vessel disease (118) and associated with cognitive dysfunction (74). In our study, we aimed at understanding the involvement of pericyte contractility in the occlusion of cerebral microvessels. In order to target the capillary network, we used microspheres of 10 μm diameter, while previously 40–70 μm-sized cholesterol crystals or 20 μm-large microspheres had been injected into the circulation of mice to block penetrating arteries or arterioles, with the aim of understanding consequent neuronal damage (72,73). Using 10 μm microbeads, we primarily occluded capillaries covered by ensheathing and mesh pericytes, while higher order capillaries had been previously targeted using 4 μm-diameter microspheres (119).

In our study, we did not observe crucial differences in the distribution of microspheres between young and old mice. Consistent with other studies, the majority of microspheres lodged in the neocortex, followed by the thalamus and the hippocampus. However, although the difference was not significant, in the hippocampus and in the white matter, higher number of microspheres were occluded in the vessels of old mice compared to young ones. It has been demonstrated that the hippocampus is sensitive to hypoxia, possibly due to microvascular differences (120); therefore, this brain region is particularly vulnerable to ageing and ageing-associated hypoperfusion. The microvascular alterations caused by ageing may be more pronounced in the hippocampus possibly due to the more microspheres being trapped in the vessels in this brain region. Such as the hippocampus, the white matter is also highly affected

by ageing. Magnetic resonance imaging studies indicate that the prevalence of white matter hyperintensities increase with age, which is associated with cognitive impairment and dementia (121,122).

We observed that pericytes reacted to vessel occlusion with increased expression of α-SMA, occasionally leading to vasoconstriction in both young and old mice. This is reminiscent of previous results indicating pericyte contraction and consequent capillary constriction in response to global cerebral ischaemia induced by middle cerebral artery occlusion (82). This reaction might probably help in isolating the damaged microvessels, limiting the consequences of BBB breakdown (79). However, vessel constriction may outlast perfusion blockage, and clamping pericytes might restrict reperfusion (80) and possibly die in rigour (20). Alternatively, pericytes might possibly also facilitate recanalization or vessel pruning (119). As a limitation of the present work, we have not assessed the direct effect of microocclusions on pericytes in vivo.

Single microocclusions presumably do not cause severe damage in the brain; however, the severity of an isolated microstroke largely depends on the local vascular topology (123). In addition, accumulating microstrokes may contribute to a progressive loss of open capillaries, which might have an even worse outcome in the ageing brain already affected by microvascular rarefaction (45) or in a possible larger ischaemic stroke.

Ischaemic stroke treatment includes thrombolysis and mechanical thrombectomy; however, hypoxia-induced contraction of mural cells, which could lead to poor prognosis, remains mostly unresolved both in larger and smaller lesions. Ischaemia-induced sustained contraction of pericytes with high α-SMA content causes persistent capillary constriction, even after reoxygenation, forming the pathophysiological basis of the no-reflow phenomenon with severe consequences on the outcome of an ischaemic attack (82). Purinergic receptors, the Ca^{2+}-gated Cl^- channel, transmembrane member 16A, and mammalian target of rapamycin complex 1 (mTORC1) were found to mediate this effect (124–126). A central component of the signalling pathway is Rho-associated protein kinase (ROCK)-dependent phosphorylation of MLC kinase, which leads to actomyosin contraction. Consistent with this, inhibitors of mTORC1, ROCK and myosin II have been shown to improve cerebral blood reperfusion following ischaemic stroke (126–128). These suggest that pericytes can be an important therapeutic target of ischaemic stroke treatment.

Out of other contractile elements, we investigated γ-actin, which was suggested to participate in the contractility of VSMCs (37). Among the six actin isoforms, β- and γ-actin are the two which are non-muscle or cytoplasmic actin isoforms (129). They differ by only four

amino acids and are expressed in both muscle and non-muscle cells (26). Expression of γ-actin has been detected in both endothelial cells (130) and pericytes (36); however, expression of this actin isoform in pericytes of the CNS has been debated (34,36). Our results clearly indicated the presence of γ-actin in microvascular endothelial cells of the brain but not in pericytes. Expression of γ-actin did not increase but slightly decreased in response to lumen obstruction.

Analysis of vascular alterations in brain metastases revealed pronounced α-SMA expression in the peritumoural microenvironment. Several studies have reported α-SMA-expressing pericytes on intratumoral vessels, linked to hypoxia, vascular leakiness, or endothelial sprouting, all of which are associated with tumour progression (131–133). However, vasoconstriction induced by high levels of tumour-derived endothelin-1 has been shown to suppress tumour growth by reducing the blood supply to cancer cells (134). Endothelin-1 has also been demonstrated to affect pericyte contractility *in vitro* and *ex vivo* (135–137), suggesting that pericytes may play an important role in tumour-related vasoconstriction. Since pericytes can contribute to processes that are either beneficial or detrimental to tumour development, their role remains uncertain.

On the other hand, in our experiments, we focused on the initial steps of metastasis formation, before tumour cells extravasate into the brain. Cancer cells arrested in cerebral capillaries spend a few days inside the vessel lumen before proceeding to transmigration through the vessel wall. In order to become isolated from the mechanical stress and possible immune attacks coming from circulation, metastatic cells induce vessel obstruction through endothelial plug formation (with a frequency of 84%), as well as vasoconstriction (in ~9% of the cases) (88). As shown here, this is probably a result of increased pericyte contractility driven by α-SMA upregulation. The underlying molecular mechanisms are still unknown. Nevertheless, tumour cells intensively communicate with cells of the NVU during the metastatic process (138).

Taken together, pericyte dysfunction contributes significantly to cerebrovascular changes associated with ageing and different pathological conditions. Pericytes actively compensate for the dysfunction by extending long processes to cover endothelial cells (59); however, pericyte remodelling is slower in the aged brain (57). Changes in the expression of contractile proteins (including ageing-induced reduction in α-SMA content and increased expression in response to microstrokes) might also be compensatory mechanisms; however, further studies are needed to clarify this question. We have also observed that obstruction of cerebral microvessels increases α-SMA expression in pericytes in both age groups, but this does not compensate for the difference in the basal expression. Increased α-SMA expression may

lead to constriction of the obstructed vessels, which probably aggravates flow heterogeneity and contributes to impaired capillary blood flow in the aged brain. In addition, we have shown that γ-actin is expressed more in endothelial cells than in pericytes; therefore, it is presumably not involved in the response of pericytes to ageing and microinfarcts. Moreover, we have also demonstrated that the contractile proteins of pericytes may play a role in the tumour development as we detected α-SMA expression surrounding the cancer cells arrested in cerebral capillaries.

IX. Summary

The NVU represents a close structural and functional relationship between cerebral microvascular cells (endothelial cells and pericytes) and neural cells (neurons and glia) having two main functions, regulation of CBF and the BBB. Among cells of the NVU, pericytes are the least well-defined and most controversial cells. They are mural cells embedded in the basement membrane of microvessels, intimately associated with endothelial and glial cells. Due to their heterogeneity, they are organized as ensheathing, mesh and thin-strand types. These latter two, together called capillary pericytes, have low levels of α-SMA, regulating basal vascular tone and applying a slow influence on CBF, while ensheathing pericytes possess more contractile protein, allowing them to robustly regulate vasoconstriction and vasodilation.

Pericytes are subject to alterations in ageing which may be even more pronounced in age-related pathologies, including microinfarcts, which usually affect a large number of vessels in the ageing brain. Age-related morphological and functional changes of the NVU, including vessel rarefaction, micro-haemorrhages, increased BBB permeability, as well as diminished CBF and reduced neurovascular coupling are the consequence of cellular and molecular changes, which involve senescence and inflamm-ageing (42,139). Pericyte dysfunction and even pericyte loss are the main components of these alterations (60); local pericyte loss results in focal capillary dilation that leads to increased flow heterogeneity (57). Pericyte dysfunction is even more pronounced in ageing-related pathologies, including neurodegenerative and ischaemic conditions (80,140). Ischaemia was shown to induce pericyte contraction that could be followed by pericyte death in rigour, which may irreversibly constrict capillaries.

Alterations in cell contractility may also contribute to age-related pericyte dysfunction; therefore, we aimed to understand changes in the expression and regulation of contractile proteins in pericytes during ageing. Additionally, changes in pericytes, especially in their expression of contractile proteins remain largely unknown in response to microinfarcts. Therefore, our second objective was to understand the changes in α-SMA expression in obstructed microvessels. Next, we hypothesized that other actin isoforms than α-SMA might be involved in the regulation of pericyte contractility. Finally, we aimed to uncover the role of pericytes in tumour cell-induced vascular changes by examining α-SMA expression in microvessels containing metastatic cells.

We obtained isolated microvessels and brain sections from young (2 to 3 months of age) and old (24 months of age) mice, as well as young and old rats. To model microinfarcts, we injected 10 μm-size microspheres into the circulation of mice resulting in the occlusion of

capillaries covered by ensheathing and mesh pericytes; while to induce brain metastasis, we delivered 4T1 cells to the mice by intracarotid injection.

We observed that α-SMA and *Acta2*, the gene encoding it, as well as TGF-β1/*Tgfb1*, the major regulator of α-SMA, decreased during ageing in cerebral microvessels. However, the unchanged CD13 (aminopeptidase N) protein levels with ageing suggest that the observed phenomenon is due to altered protein expression rather than changes in pericyte number. In the vicinity of the microspheres stalled in the capillaries, expression of α-SMA increased significantly in both ensheathing and especially in mesh pericytes, both in young (2 to 3 months of age) and old (24 months of age) mice. On the other hand, γ-actin was detected in endothelial cells, but not in pericytes, and decreased in microvessels of microsphere-containing hemispheres. Furthermore, while investigating the vascular changes in brain metastasis, we found high α-SMA expression in the vessels containing tumour cells.

Altogether, our data show that obstruction of cerebral microvessels increases α-SMA expression in pericytes in both age groups, but this does not compensate for the lower expression of the contractile protein in old animals. Increased α-SMA expression may lead to constriction of the obstructed vessels probably aggravating flow heterogeneity in the aged brain and in brain metastasis. While pericyte contractility appears to be detrimental in the context of microinfarcts, its role in brain metastasis—where metastatic cells become isolated due to vessel obstruction—remains less clear. In conclusion, brain pericytes are key players in regulating ageing-associated ischaemic responses; therefore, targeting pericytes may offer new therapeutic opportunities for ischaemic stroke.

X. Acknowledgements

First and foremost, I would like to express my deepest gratitude to my supervisor, Imola Wilhelm, for her guidance, support, and encouragement throughout my research and the writing of this dissertation. Her passion for science has been truly inspiring to me. I am especially thankful for her openness to new ideas and her insightful feedback. Her support helped me to develop both professionally and personally, and it enabled me to grow into a more confident and self-reliant researcher.

I am also sincerely grateful to István Krizbai, head of the Neurovascular Unit Research Group for providing me with the opportunity to carry out my research in his laboratory, and for his support, including the opportunity to participate in international conferences.

I would like to express my heartfelt thanks to all my colleagues in the Neurovascular Unit Research Group for their help, the useful discussions, and the good atmosphere that made this journey more enjoyable. In particular, I am deeply grateful to Ádám Mészáros for his invaluable help in my work, which contributed greatly to the completion of this research. I would also like to thank Attila Farkas, Csilla Fazakas and Mónika Krecsmarik for their contribution and help during my work. I would like to express my special thanks to Tamás Dudás and Valentina Nagy for their encouragement and emotional support, which helped me through the more difficult periods of my studies. I am also grateful to my present and former colleagues, Tejal Shreeya, Lam Tri Duc, Kinga Mészáros-Molnár, János Haskó, Ádám Nyúl-Tóth, Maryam Naeem, Lebogang Duba Ledile, and Rabiya Bano for creating a friendly and supportive work environment throughout these years.

I would like to thank Anca Hermenean's research group at the Vasile Goldiș Western University of Arad for generously providing the experimental animals and allowing us to carry out part of the study in their laboratory. I am especially grateful to Cornel Balta, Hildegard Herman, and Bianca Maria Mladin for their kind support and assistance during the experimental work.

Last but not least, I would like to thank my family and friends for continuous support throughout this period. Their patience and help have been invaluable to me during these years.

My work was supported by a research scholarship from the New National Excellence Program of the Ministry of Human Capacities (ÚNKP-23-3 -SZTE-287), for which I am truly grateful.

XI. References

1. Schaeffer S, Iadecola C. Revisiting the neurovascular unit. Nat Neurosci. 2021 Sep;24(9):1198–209.

2. Zhao Z, Nelson AR, Betsholtz C, Zlokovic BV. Establishment and Dysfunction of the Blood-Brain Barrier. Cell. 2015 Nov;163(5):1064–78.

3. Iadecola C. The Neurovascular Unit Coming of Age: A Journey through Neurovascular Coupling in Health and Disease. Neuron. 2017 Sep;96(1):17–42.

4. Bell AH, Miller SL, Castillo-Melendez M, Malhotra A. The Neurovascular Unit: Effects of Brain Insults During the Perinatal Period. Front Neurosci. 2020 Jan 22;13:1452.

5. Nippert AR, Biesecker KR, Newman EA. Mechanisms Mediating Functional Hyperemia in the Brain. The Neuroscientist. 2018 Feb;24(1):73–83.

6. Carmignoto G, Gómez-Gonzalo M. The contribution of astrocyte signalling to neurovascular coupling. Brain Res Rev. 2010 May;63(1–2):138–48.

7. Abbott NJ, Rönnbäck L, Hansson E. Astrocyte–endothelial interactions at the blood–brain barrier. Nat Rev Neurosci. 2006 Jan 1;7(1):41–53.

8. Attwell D, Mishra A, Hall CN, O'Farrell FM, Dalkara T. What is a pericyte? J Cereb Blood Flow Metab. 2016 Feb;36(2):451–5.

9. Winkler EA, Bell RD, Zlokovic BV. Pericyte-specific expression of PDGF beta receptor in mouse models with normal and deficient PDGF beta receptor signaling. Mol Neurodegener. 2010 Dec;5(1):32.

10. Hartmann DA, Underly RG, Grant RI, Watson AN, Lindner V, Shih AY. Pericyte structure and distribution in the cerebral cortex revealed by high-resolution imaging of transgenic mice. Neurophotonics. 2015 May 27;2(4):041402.

11. Armulik A, Genové G, Mäe M, Nisancioglu MH, Wallgard E, Niaudet C, et al. Pericytes regulate the blood–brain barrier. Nature. 2010 Nov;468(7323):557–61.

12. Grant RI, Hartmann DA, Underly RG, Berthiaume AA, Bhat NR, Shih AY. Organizational hierarchy and structural diversity of microvascular pericytes in adult mouse cortex. J Cereb Blood Flow Metab. 2019 Mar;39(3):411–25.

13. Hill RA, Tong L, Yuan P, Murikinati S, Gupta S, Grutzendler J. Regional Blood Flow in the Normal and Ischemic Brain Is Controlled by Arteriolar Smooth Muscle Cell Contractility and Not by Capillary Pericytes. Neuron. 2015 Jul;87(1):95–110.

14. Vontell D, Armulik A, Betsholtz C. Pericytes and vascular stability. Exp Cell Res. 2006 Mar 10;312(5):623–9.

15. Daneman R, Zhou L, Kebede AA, Barres BA. Pericytes are required for blood–brain barrier integrity during embryogenesis. Nature. 2010 Nov;468(7323):562–6.

16. Hurtado-Alvarado G, Cabañas-Morales AM, Gómez-Gónzalez B. Pericytes: brain-immune interface modulators. Front Integr Neurosci [Internet]. 2014 [cited 2024 Jun 12];7. Available from: http://journal.frontiersin.org/article/10.3389/fnint.2013.00080/abstract

17. Balabanov R, Beaumont T, Dore-Duffy P. Role of central nervous system microvascular pericytes in activation of antigen-primed splenic T-lymphocytes. J Neurosci Res. 1999 Mar 1;55(5):578–87.

18. Kovac A, Erickson MA, Banks WA. Brain microvascular pericytes are immunoactive in culture: cytokine, chemokine, nitric oxide, and LRP-1 expression in response to lipopolysaccharide. J Neuroinflammation. 2011 Dec;8(1):139.

19. Hamilton NB. Pericyte-mediated regulation of capillary diameter: a component of neurovascular coupling in health and disease. Front Neuroenergetics [Internet]. 2010 [cited 2024 Jun 13];2. Available from: http://journal.frontiersin.org/article/10.3389/fnene.2010.00005/abstract

20. Hall CN, Reynell C, Gesslein B, Hamilton NB, Mishra A, Sutherland BA, et al. Capillary pericytes regulate cerebral blood flow in health and disease. Nature. 2014 Apr;508(7494):55–60.

21. Hartmann DA, Berthiaume AA, Grant RI, Harrill SA, Koski T, Tieu T, et al. Brain capillary pericytes exert a substantial but slow influence on blood flow. Nat Neurosci. 2021 May;24(5):633–45.

22. Kisler K, Nelson AR, Rege SV, Ramanathan A, Wang Y, Ahuja A, et al. Pericyte degeneration leads to neurovascular uncoupling and limits oxygen supply to brain. Nat Neurosci. 2017 Mar;20(3):406–16.

23. Hartmann DA, Coelho-Santos V, Shih AY. Pericyte Control of Blood Flow Across Microvascular Zones in the Central Nervous System. Annu Rev Physiol. 2022 Feb 10;84(1):331–54.

24. Peppiatt CM, Howarth C, Mobbs P, Attwell D. Bidirectional control of CNS capillary diameter by pericytes. Nature. 2006 Oct;443(7112):700–4.

25. Murrell M, Oakes PW, Lenz M, Gardel ML. Forcing cells into shape: the mechanics of actomyosin contractility. Nat Rev Mol Cell Biol. 2015 Aug;16(8):486–98.

26. Perrin BJ, Ervasti JM. The actin gene family: Function follows isoform. Cytoskeleton. 2010 Oct;67(10):630–4.

27. Arora AS, Huang HL, Singh R, Narui Y, Suchenko A, Hatano T, et al. Structural insights into actin isoforms. eLife. 2023 Feb 15;12:e82015.

28. Pepper I, Galkin VE. Actomyosin Complex. In: Harris JR, Marles-Wright J, editors. Macromolecular Protein Complexes IV [Internet]. Cham: Springer International Publishing; 2022 [cited 2024 Jun 20]. p. 421–70. (Subcellular Biochemistry; vol. 99). Available from: https://link.springer.com/10.1007/978-3-031-00793-4_14

29. Foth BJ, Goedecke MC, Soldati D. New insights into myosin evolution and classification. Proc Natl Acad Sci. 2006 Mar 7;103(10):3681–6.

30. Webb RC. SMOOTH MUSCLE CONTRACTION AND RELAXATION. Adv Physiol Educ. 2003 Dec;27(4):201–6.

31. Vanlandewijck M, He L, Mäe MA, Andrae J, Ando K, Del Gaudio F, et al. A molecular atlas of cell types and zonation in the brain vasculature. Nature. 2018 Feb 22;554(7693):475–80.

32. Yao Z, Van Velthoven CTJ, Kunst M, Zhang M, McMillen D, Lee C, et al. A high-resolution transcriptomic and spatial atlas of cell types in the whole mouse brain. Nature. 2023 Dec 14;624(7991):317–32.

33. Gonzales AL, Klug NR, Moshkforoush A, Lee JC, Lee FK, Shui B, et al. Contractile pericytes determine the direction of blood flow at capillary junctions. Proc Natl Acad Sci. 2020 Oct 27;117(43):27022–33.

34. Alarcon-Martinez L, Yilmaz-Ozcan S, Yemisci M, Schallek J, Kılıç K, Can A, et al. Capillary pericytes express α-smooth muscle actin, which requires prevention of filamentous-actin depolymerization for detection. eLife. 2018 Mar 21;7:e34861.

35. Pernier J, Kusters R, Bousquet H, Lagny T, Morchain A, Joanny JF, et al. Myosin 1b is an actin depolymerase. Nat Commun. 2019 Nov 15;10(1):5200.

36. DeNofrio D, Hoock TC, Herman IM. Functional sorting of actin isoforms in microvascular pericytes. J Cell Biol. 1989 Jul 1;109(1):191–202.

37. Kim HR, Gallant C, Leavis PC, Gunst SJ, Morgan KG. Cytoskeletal remodeling in differentiated vascular smooth muscle is actin isoform dependent and stimulus dependent. Am J Physiol-Cell Physiol. 2008 Sep;295(3):C768–78.

38. Verbeek MM. Induction of alpha-smooth muscle actin expression in cultured human brain pericytes by transforming growth factor-beta 1. Am J Pathol. 1994;

39. Hu B, Wu Z, Phan SH. Smad3 Mediates Transforming Growth Factor-β–Induced α-Smooth Muscle Actin Expression. Am J Respir Cell Mol Biol. 2003 Sep;29(3):397–404.

40. Hautmann MB, Madsen CS, Owens GK. A Transforming Growth Factor β (TGFβ) Control Element Drives TGFβ-induced Stimulation of Smooth Muscle α-Actin Gene Expression in Concert with Two CArG Elements. J Biol Chem. 1997 Apr;272(16):10948–56.

41. Perrella MA, Jain MK, Lee ME. Role of TGF-β in Vascular Development and Vascular Reactivity. Miner Electrolyte Metab. 1998;24(2–3):136–43.

42. Wilhelm I, Nyúl-Tóth Á, Kozma M, Farkas AE, Krizbai IA. Role of pattern recognition receptors of the neurovascular unit in inflamm-aging. Am J Physiol-Heart Circ Physiol. 2017 Nov 1;313(5):H1000–12.

43. Banks WA, Reed MJ, Logsdon AF, Rhea EM, Erickson MA. Healthy aging and the blood–brain barrier. Nat Aging. 2021 Mar 15;1(3):243–54.

44. Nagata K, Yamazaki T, Takano D, Maeda T, Fujimaki Y, Nakase T, et al. Cerebral circulation in aging. Ageing Res Rev. 2016 Sep;30:49–60.

45. Nyúl-Tóth Á, Tarantini S, DelFavero J, Yan F, Balasubramanian P, Yabluchanskiy A, et al. Demonstration of age-related blood-brain barrier disruption and cerebromicrovascular rarefaction in mice by longitudinal intravital two-photon microscopy and optical coherence tomography. Am J Physiol-Heart Circ Physiol. 2021 Apr 1;320(4):H1370–92.

46. Knox EG, Aburto MR, Clarke G, Cryan JF, O'Driscoll CM. The blood-brain barrier in aging and neurodegeneration. Mol Psychiatry. 2022 Jun;27(6):2659–73.

47. Bennett HC, Zhang Q, Wu Y ting, Manjila SB, Chon U, Shin D, et al. Aging drives cerebrovascular network remodeling and functional changes in the mouse brain. Nat Commun. 2024 Jul 30;15(1):6398.

48. Lowerison MR, Sekaran NVC, Zhang W, Dong Z, Chen X, Llano DA, et al. Aging-related cerebral microvascular changes visualized using ultrasound localization microscopy in the living mouse. Sci Rep. 2022 Jan 12;12(1):619.

49. Elahy M, Jackaman C, Mamo JC, Lam V, Dhaliwal SS, Giles C, et al. Blood–brain barrier dysfunction developed during normal aging is associated with inflammation and loss of tight junctions but not with leukocyte recruitment. Immun Ageing. 2015 Dec;12(1):2.

50. Ceafalan LC, Fertig TE, Gheorghe TC, Hinescu ME, Popescu BO, Pahnke J, et al. Age-related ultrastructural changes of the basement membrane in the mouse blood-brain barrier. J Cell Mol Med. 2019 Feb;23(2):819–27.

51. Farkas E, De Vos RAI, Donka G, Jansen Steur EN, Mihály A, Luiten PGM. Age-related microvascular degeneration in the human cerebral periventricular white matter. Acta Neuropathol (Berl). 2006 Feb;111(2):150–7.

52. Poels MMF, Vernooij MW, Ikram MA, Hofman A, Krestin GP, Van Der Lugt A, et al. Prevalence and Risk Factors of Cerebral Microbleeds: An Update of the Rotterdam Scan Study. Stroke [Internet]. 2010 Oct [cited 2025 Apr 14];41(10_suppl_1). Available from: https://www.ahajournals.org/doi/10.1161/STROKEAHA.110.595181

53. Sumbria RK, Grigoryan MM, Vasilevko V, Paganini-Hill A, Kilday K, Kim R, et al. Aging exacerbates development of cerebral microbleeds in a mouse model. J Neuroinflammation. 2018 Dec;15(1):69.

54. Franceschi C, Garagnani P, Parini P, Giuliani C, Santoro A. Inflammaging: a new immune–metabolic viewpoint for age-related diseases. Nat Rev Endocrinol. 2018 Oct;14(10):576–90.

55. Mészáros Á, Molnár K, Nógrádi B, Hernádi Z, Nyúl-Tóth Á, Wilhelm I, et al. Neurovascular Inflammaging in Health and Disease. Cells. 2020 Jul 4;9(7):1614.

56. Ding R, Hase Y, Burke M, Foster V, Stevenson W, Polvikoski T, et al. Loss with ageing but preservation of frontal cortical capillary pericytes in post-stroke dementia, vascular dementia and Alzheimer's disease. Acta Neuropathol Commun. 2021 Dec;9(1):130.

57. Berthiaume AA, Schmid F, Stamenkovic S, Coelho-Santos V, Nielson CD, Weber B, et al. Pericyte remodeling is deficient in the aged brain and contributes to impaired capillary flow and structure. Nat Commun. 2022 Oct 7;13(1):5912.

58. Watson AN, Berthiaume AA, Faino AV, McDowell KP, Bhat NR, Hartmann DA, et al. Mild pericyte deficiency is associated with aberrant brain microvascular flow in aged PDGFRβ+/- mice. J Cereb Blood Flow Metab Off J Int Soc Cereb Blood Flow Metab. 2020;40(12):2387–400.

59. Berthiaume AA, Hartmann DA, Majesky MW, Bhat NR, Shih AY. Pericyte Structural Remodeling in Cerebrovascular Health and Homeostasis. Front Aging Neurosci. 2018 Jul 17;10:210.

60. Bell RD, Winkler EA, Sagare AP, Singh I, LaRue B, Deane R, et al. Pericytes Control Key Neurovascular Functions and Neuronal Phenotype in the Adult Brain and during Brain Aging. Neuron. 2010 Nov;68(3):409–27.

61. Nikolakopoulou AM, Montagne A, Kisler K, Dai Z, Wang Y, Huuskonen MT, et al. Pericyte loss leads to circulatory failure and pleiotrophin depletion causing neuron loss. Nat Neurosci. 2019 Jul;22(7):1089–98.

62. Cicognola C, Mattsson-Carlgren N, Van Westen D, Zetterberg H, Blennow K, Palmqvist S, et al. Associations of CSF PDGFRβ With Aging, Blood-Brain Barrier Damage, Neuroinflammation, and Alzheimer Disease Pathologic Changes. Neurology [Internet]. 2023 Jul 4 [cited 2024 Aug 5];101(1). Available from: https://www.neurology.org/doi/10.1212/WNL.0000000000207358

63. Cai C, Zambach SA, Grubb S, Tao L, He C, Lind BL, et al. Impaired dynamics of precapillary sphincters and pericytes at first-order capillaries predict reduced neurovascular function in the aging mouse brain. Nat Aging. 2023 Jan 26;3(2):173–84.

64. Smith EE, Schneider JA, Wardlaw JM, Greenberg SM. Cerebral microinfarcts: the invisible lesions. Lancet Neurol. 2012 Mar;11(3):272–82.

65. Van Veluw SJ, Shih AY, Smith EE, Chen C, Schneider JA, Wardlaw JM, et al. Detection, risk factors, and functional consequences of cerebral microinfarcts. Lancet Neurol. 2017 Sep;16(9):730–40.

66. Kövari E, Herrmann FR, Gold G, Hof PR, Charidimou A. Association of cortical microinfarcts and cerebral small vessel pathology in the ageing brain. Neuropathol Appl Neurobiol. 2017 Oct;43(6):505–13.

67. Soontornniyomkij V, Lynch MD, Mermash S, Pomakian J, Badkoobehi H, Clare R, et al. Cerebral microinfarcts associated with severe cerebral beta-amyloid angiopathy. Brain Pathol Zurich Switz. 2010 Mar;20(2):459–67.

68. Bladin CF, Chambers BR. Clinical features, pathogenesis, and computed tomographic characteristics of internal watershed infarction. Stroke. 1993 Dec;24(12):1925–32.

69. Ferro DA, Mutsaerts HJ, Hilal S, Kuijf HJ, Petersen ET, Petr J, et al. Cortical microinfarcts in memory clinic patients are associated with reduced cerebral perfusion. J Cereb Blood Flow Metab. 2020 Sep;40(9):1869–78.

70. Suter OC, Sunthorn T, Kraftsik R, Straubel J, Darekar P, Khalili K, et al. Cerebral Hypoperfusion Generates Cortical Watershed Microinfarcts in Alzheimer Disease. Stroke. 2002 Aug;33(8):1986–92.

71. Russell D. Cerebral microemboli and cognitive impairment. J Neurol Sci. 2002 Nov;203–204:211–4.

72. Silasi G, She J, Boyd JD, Xue S, Murphy TH. A Mouse Model of Small-Vessel Disease that Produces Brain-Wide-Identified Microocclusions and Regionally Selective Neuronal Injury. J Cereb Blood Flow Metab. 2015 May;35(5):734–8.

73. Wang M, Iliff JJ, Liao Y, Chen MJ, Shinseki MS, Venkataraman A, et al. Cognitive Deficits and Delayed Neuronal Loss in a Mouse Model of Multiple Microinfarcts. J Neurosci. 2012 Dec 12;32(50):17948–60.

74. Brundel M, De Bresser J, Van Dillen JJ, Kappelle LJ, Biessels GJ. Cerebral Microinfarcts: A Systematic Review of Neuropathological Studies. J Cereb Blood Flow Metab. 2012 Mar;32(3):425–36.

75. Kövari E, Gold G, Herrmann FR, Canuto A, Hof PR, Michel JP, et al. Cortical Microinfarcts and Demyelination Significantly Affect Cognition in Brain Aging. Stroke. 2004 Feb;35(2):410–4.

76. Ince PG, Minett T, Forster G, Brayne C, Wharton SB, the Medical Research Council Cognitive Function and Ageing Neuropathology Study. Microinfarcts in an older population-representative brain donor cohort (MRC CFAS): Prevalence, relation to dementia and mobility, and implications for the evaluation of cerebral Small Vessel Disease. Neuropathol Appl Neurobiol. 2017 Aug;43(5):409–18.

77. Ballard C, McKeith I, O'Brien J, Kalaria R, Jaros E, Ince P, et al. Neuropathological Substrates of Dementia and Depression in Vascular Dementia, with a Particular Focus on Cases with Small Infarct Volumes. Dement Geriatr Cogn Disord. 2000;11(2):59–65.

78. Conklin J, Silver FL, Mikulis DJ, Mandell DM. Are acute infarcts the cause of leukoaraiosis? Brain mapping for 16 consecutive weeks. Ann Neurol. 2014 Dec;76(6):899–904.

79. Fernandez-Klett F, Priller J. Diverse Functions of Pericytes in Cerebral Blood Flow Regulation and Ischemia. J Cereb Blood Flow Metab. 2015 Jun;35(6):883–7.

80. Whitehead B, Karelina K, Weil ZM. Pericyte dysfunction is a key mediator of the risk of cerebral ischemia. J Neurosci Res. 2023 Dec;101(12):1840–8.

81. Neuhaus AA, Couch Y, Sutherland BA, Buchan AM. Novel method to study pericyte contractility and responses to ischaemia *in vitro* using electrical impedance. J Cereb Blood Flow Metab. 2017 Jun;37(6):2013–24.

82. Yemisci M, Gursoy-Ozdemir Y, Vural A, Can A, Topalkara K, Dalkara T. Pericyte contraction induced by oxidative-nitrative stress impairs capillary reflow despite successful opening of an occluded cerebral artery. Nat Med. 2009 Sep;15(9):1031–7.

83. Majno G, Ames A, Chiang J, Wright RL. NO REFLOW AFTER CEREBRAL ISCHÆMIA. The Lancet. 1967 Sep;290(7515):569–70.

84. Ames A, Wright RL, Kowada M, Thurston JM, Majno G. Cerebral ischemia. II. The no-reflow phenomenon. Am J Pathol. 1968 Feb;52(2):437–53.

85. Sun F, Zhou J, Chen X, Yang T, Wang G, Ge J, et al. No-reflow after recanalization in ischemic stroke: From pathomechanisms to therapeutic strategies. J Cereb Blood Flow Metab. 2024 Jun;44(6):857–80.

86. Underly RG, Levy M, Hartmann DA, Grant RI, Watson AN, Shih AY. Pericytes as Inducers of Rapid, Matrix Metalloproteinase-9-Dependent Capillary Damage during Ischemia. J Neurosci. 2017 Jan 4;37(1):129–40.

87. Bai Y, Zhu X, Chao J, Zhang Y, Qian C, Li P, et al. Pericytes Contribute to the Disruption of the Cerebral Endothelial Barrier via Increasing VEGF Expression: Implications for Stroke. Germain S, editor. PLOS ONE. 2015 Apr 17;10(4):e0124362.

88. Haskó J, Fazakas C, Molnár K, Mészáros Á, Patai R, Szabó G, et al. Response of the neurovascular unit to brain metastatic breast cancer cells. Acta Neuropathol Commun. 2019 Dec;7(1):133.

89. Seoane J, De Mattos-Arruda L. Brain metastasis: New opportunities to tackle therapeutic resistance. Mol Oncol. 2014 Sep;8(6):1120–31.

90. Wilhelm I, Molnár J, Fazakas C, Haskó J, Krizbai I. Role of the Blood-Brain Barrier in the Formation of Brain Metastases. Int J Mol Sci. 2013 Jan 11;14(1):1383–411.

91. Molnár K, Mészáros Á, Fazakas C, Kozma M, Győri F, Reisz Z, et al. Pericyte-secreted IGF2 promotes breast cancer brain metastasis formation. Mol Oncol. 2020 Sep;14(9):2040–57.

92. Sun H, Guo D, Su Y, Yu D, Wang Q, Wang T, et al. Hyperplasia of Pericytes Is One of the Main Characteristics of Microvascular Architecture in Malignant Glioma. Camussi G, editor. PLoS ONE. 2014 Dec 5;9(12):e114246.

93. Caspani EM, Crossley PH, Redondo-Garcia C, Martinez S. Glioblastoma: A Pathogenic Crosstalk between Tumor Cells and Pericytes. Castro MG, editor. PLoS ONE. 2014 Jul 17;9(7):e101402.

94. Mitchell D, Ibrahim S, Gusterson BA. Improved immunohistochemical localization of tissue antigens using modified methacarn fixation. J Histochem Cytochem. 1985 May;33(5):491–5.

95. Tang Y, Urs S, Boucher J, Bernaiche T, Venkatesh D, Spicer DB, et al. Notch and Transforming Growth Factor-β (TGFβ) Signaling Pathways Cooperatively Regulate Vascular Smooth Muscle Cell Differentiation. J Biol Chem. 2010 Jun;285(23):17556–63.

96. Wu CF, Chiang WC, Lai CF, Chang FC, Chen YT, Chou YH, et al. Transforming Growth Factor β-1 Stimulates Profibrotic Epithelial Signaling to Activate Pericyte-Myofibroblast Transition in Obstructive Kidney Fibrosis. Am J Pathol. 2013 Jan;182(1):118–31.

97. Erdener ŞE, Küreli G, Dalkara T. Contractile apparatus in CNS capillary pericytes. Neurophotonics [Internet]. 2022 Jan 24 [cited 2024 Jun 17];9(02). Available from: https://www.spiedigitallibrary.org/journals/neurophotonics/volume-9/issue-02/021904/Contractile-apparatus-in-CNS-capillary-pericytes/10.1117/1.NPh.9.2.021904.full

98. Csipo T, Mukli P, Lipecz A, Tarantini S, Bahadli D, Abdulhussein O, et al. Assessment of age-related decline of neurovascular coupling responses by functional near-infrared spectroscopy (fNIRS) in humans. GeroScience. 2019 Oct;41(5):495–509.

99. Levit A, Hachinski V, Whitehead SN. Neurovascular unit dysregulation, white matter disease, and executive dysfunction: the shared triad of vascular cognitive impairment and Alzheimer disease. GeroScience. 2020 Apr;42(2):445–65.

100. Sengillo JD, Winkler EA, Walker CT, Sullivan JS, Johnson M, Zlokovic BV. Deficiency in Mural Vascular Cells Coincides with Blood–Brain Barrier Disruption in A lzheimer's Disease. Brain Pathol. 2013 May;23(3):303–10.

101. Montagne A, Barnes SR, Sweeney MD, Halliday MR, Sagare AP, Zhao Z, et al. Blood-Brain Barrier Breakdown in the Aging Human Hippocampus. Neuron. 2015 Jan;85(2):296–302.

102. Wang Y, Pan L, Moens CB, Appel B. Notch3 establishes brain vascular integrity by regulating pericyte number. Development. 2014 Jan 15;141(2):307–17.

103. Nadeem T, Bogue W, Bigit B, Cuervo H. Deficiency of Notch signaling in pericytes results in arteriovenous malformations. JCI Insight. 2020 Nov 5;5(21):e125940.

104. Romay MC, Knutsen RH, Ma F, Mompeón A, Hernandez GE, Salvador J, et al. Age-related loss of Notch3 underlies brain vascular contractility deficiencies, glymphatic dysfunction, and neurodegeneration in mice. J Clin Invest. 2024 Jan 16;134(2):e166134.

105. Stopa EG, Butala P, Salloway S, Johanson CE, Gonzalez L, Tavares R, et al. Cerebral Cortical Arteriolar Angiopathy, Vascular Beta-Amyloid, Smooth Muscle Actin, Braak Stage, and *APOE* Genotype. Stroke. 2008 Mar;39(3):814–21.

106. Merlini M, Wanner D, Nitsch RM. Tau pathology-dependent remodelling of cerebral arteries precedes Alzheimer's disease-related microvascular cerebral amyloid angiopathy. Acta Neuropathol (Berl). 2016 May;131(5):737–52.

107. Nikolakopoulou AM, Zhao Z, Montagne A, Zlokovic BV. Regional early and progressive loss of brain pericytes but not vascular smooth muscle cells in adult mice with disrupted platelet-derived growth factor receptor-β signaling. Deli MA, editor. PLOS ONE. 2017 Apr 25;12(4):e0176225.

108. Hase Y, Ding R, Harrison G, Hawthorne E, King A, Gettings S, et al. White matter capillaries in vascular and neurodegenerative dementias. Acta Neuropathol Commun. 2019 Dec;7(1):16.

109. Wagner M, Jurcoane A, Volz S, Magerkurth J, Zanella FE, Neumann-Haefelin T, et al. Age-Related Changes of Cerebral Autoregulation: New Insights with Quantitative T2′-Mapping and Pulsed Arterial Spin-Labeling MR Imaging. Am J Neuroradiol. 2012 Dec;33(11):2081–7.

110. Papetti M, Shujath J, Riley KN, Herman IM. FGF-2 Antagonizes the TGF-β1-Mediated Induction of Pericyte α-Smooth Muscle Actin Expression: A Role for Myf-5 and Smad-Mediated Signaling Pathways. Investig Opthalmology Vis Sci. 2003 Nov 1;44(11):4994.

111. Armulik A, Abramsson A, Betsholtz C. Endothelial/Pericyte Interactions. Circ Res. 2005 Sep 16;97(6):512–23.

112. Dohgu S, Takata F, Yamauchi A, Nakagawa S, Egawa T, Naito M, et al. Brain pericytes contribute to the induction and up-regulation of blood–brain barrier functions through transforming growth factor-β production. Brain Res. 2005 Mar;1038(2):208–15.

113. Fu J, Li L, Huo D, Zhi S, Yang R, Yang B, et al. Astrocyte-Derived TGFβ1 Facilitates Blood–Brain Barrier Function via Non-Canonical Hedgehog Signaling in Brain Microvascular Endothelial Cells. Brain Sci. 2021 Jan 8;11(1):77.

114. Krizbai IA, Gasparics Á, Nagyőszi P, Fazakas C, Molnár J, Wilhelm I, et al. Endothelial-Mesenchymal Transition of Brain Endothelial Cells: Possible Role during Metastatic Extravasation. Languino LR, editor. PLOS ONE. 2015 Mar 5;10(3):e0119655.

115. Chen J, Luo Y, Hui H, Cai T, Huang H, Yang F, et al. CD146 coordinates brain endothelial cell–pericyte communication for blood–brain barrier development. Proc Natl Acad Sci [Internet]. 2017 Sep 5 [cited 2024 Oct 25];114(36). Available from: https://pnas.org/doi/full/10.1073/pnas.1710848114

116. Chen MB, Yang AC, Yousef H, Lee D, Chen W, Schaum N, et al. Brain Endothelial Cells Are Exquisite Sensors of Age-Related Circulatory Cues. Cell Rep. 2020 Mar;30(13):4418-4432.e4.

117. Westover MB, Bianchi MT, Yang C, Schneider JA, Greenberg SM. Estimating cerebral microinfarct burden from autopsy samples. Neurology. 2013 Apr 9;80(15):1365–9.

118. De Silva TM, Faraci FM. Contributions of Aging to Cerebral Small Vessel Disease. Annu Rev Physiol. 2020 Feb 10;82(1):275–95.

119. Reeson P, Choi K, Brown CE. VEGF signaling regulates the fate of obstructed capillaries in mouse cortex. eLife. 2018 Apr 26;7:e33670.

120. Shaw K, Bell L, Boyd K, Grijseels DM, Clarke D, Bonnar O, et al. Neurovascular coupling and oxygenation are decreased in hippocampus compared to neocortex because of microvascular differences. Nat Commun. 2021 May 27;12(1):3190.

121. De Leeuw FE. Prevalence of cerebral white matter lesions in elderly people: a population based magnetic resonance imaging study. The Rotterdam Scan Study. J Neurol Neurosurg Psychiatry. 2001 Jan 1;70(1):9–14.

122. Ferro JM, Madureira S. Age-related white matter changes and cognitive impairment. J Neurol Sci. 2002 Nov;203–204:221–5.

123. Schmid F, Conti G, Jenny P, Weber B. The severity of microstrokes depends on local vascular topology and baseline perfusion. eLife. 2021 May 18;10:e60208.

124. Cai C, Fordsmann JC, Jensen SH, Gesslein B, Lønstrup M, Hald BO, et al. Stimulation-induced increases in cerebral blood flow and local capillary vasoconstriction depend on conducted vascular responses. Proc Natl Acad Sci [Internet]. 2018 Jun 19 [cited 2025 Jan 15];115(25). Available from: https://pnas.org/doi/full/10.1073/pnas.1707702115

125. Korte N, Ilkan Z, Pearson CL, Pfeiffer T, Singhal P, Rock JR, et al. The Ca2+-gated channel TMEM16A amplifies capillary pericyte contraction and reduces cerebral blood flow after ischemia. J Clin Invest. 2022 May 2;132(9):e154118.

126. Beard DJ, Brown LS, Morris GP, Couch Y, Adriaanse BA, Karali CS, et al. Rapamycin Treatment Reduces Brain Pericyte Constriction in Ischemic Stroke. Transl Stroke Res [Internet]. 2024 Sep 27 [cited 2025 Feb 24]; Available from: https://link.springer.com/10.1007/s12975-024-01298-x

127. Rikitake Y, Kim HH, Huang Z, Seto M, Yano K, Asano T, et al. Inhibition of Rho Kinase (ROCK) Leads to Increased Cerebral Blood Flow and Stroke Protection. Stroke. 2005 Oct;36(10):2251–7.

128. Pénzes M, Túrós D, Máthé D, Szigeti K, Hegedűs N, Rauscher AÁ, et al. Direct myosin-2 inhibition enhances cerebral perfusion resulting in functional improvement after ischemic stroke. Theranostics. 2020;10(12):5341–56.

129. Heissler SM, Chinthalapudi K. Structural and functional mechanisms of actin isoforms. FEBS J. 2024 May 23;febs.17153.

130. Dugina VB, Shagieva GS, Shakhov AS, Alieva IB. The Cytoplasmic Actins in the Regulation of Endothelial Cell Function. Int J Mol Sci. 2021 Jul 22;22(15):7836.

131. Bugyik E, Dezső K, Reiniger L, László V, Tóvári J, Tímár J, et al. Lack of Angiogenesis in Experimental Brain Metastases. J Neuropathol Exp Neurol. 2011 Nov;70(11):979–91.

132. Natarajan V, Ha S, Delgado A, Jacobson R, Alhalhooly L, Choi Y, et al. Acquired αSMA Expression in Pericytes Coincides with Aberrant Vascular Structure and Function in Pancreatic Ductal Adenocarcinoma. Cancers. 2022 May 16;14(10):2448.

133. Morikawa S, Baluk P, Kaidoh T, Haskell A, Jain RK, McDonald DM. Abnormalities in Pericytes on Blood Vessels and Endothelial Sprouts in Tumors. Am J Pathol. 2002 Mar;160(3):985–1000.

134. Weydert C, Esser A, Mejia R, Drake J, Barnes J, Henry M. Endothelin-1 inhibits prostate cancer growth in vivo through vasoconstriction of tumor-feeding arterioles. Cancer Biol Ther. 2009 Apr 15;8(8):720–9.

135. Dodge AB, Hechtman HB, Shepro D. Microvascular endothelial-derived autacoids regulate pericyte contractility. Cell Motil. 1991 Jan;18(3):180–8.

136. Chakravarthy U, Gardiner TA, Anderson P, Archer DB, Trimble ER. The effect of endothelin 1 on the retinal microvascular pericyte. Microvasc Res. 1992 May;43(3):241–54.

137. Schönfelder U, Hofer A, Paul M, Funk RHW. In SituObservation of Living Pericytes in Rat Retinal Capillaries. Microvasc Res. 1998 Jul;56(1):22–9.

138. Wilhelm I, Fazakas C, Molnár K, Végh AG, Haskó J, Krizbai IA. Foe or friend? Janus-faces of the neurovascular unit in the formation of brain metastases. J Cereb Blood Flow Metab. 2018 Apr;38(4):563–87.

139. Csiszar A, Ungvari A, Patai R, Gulej R, Yabluchanskiy A, Benyo Z, et al. Atherosclerotic burden and cerebral small vessel disease: exploring the link through microvascular aging and cerebral microhemorrhages. GeroScience [Internet]. 2024 Apr 19 [cited 2024 Aug 5]; Available from: https://link.springer.com/10.1007/s11357-024-01139-7

140. Bennett HC, Kim Y. Pericytes Across the Lifetime in the Central Nervous System. Front Cell Neurosci. 2021 Mar 12;15:627291.

Appendix

Co-author certification

I, myself as a corresponding author of the following publication declare that the authors have no conflict of interest, and Fanni Győri, Ph.D. candidate had significant contribution to the jointly published research. The results discussed in her thesis were not used and not intended to be used in any other qualification process for obtaining a PhD degree.

....

date Imola Wilhelm, author

The publication(s) relevant to the applicant's thesis: Wilhelm, I., **Győri, F.**, Dudás, T., Nagy, V., Shreeya, T., Krecsmarik, M., Farkas, A. E., Fazakas, C., Krizbai, I. A. (2025). Eppur si muove: The dynamic brain pericyte (manuscript under review in *Fluids and Barriers of the CNS*)